Biochimica et Biophysica Acta 1847 (2015) 19–34

Contents lists available at ScienceDirect

Biochimica et Biophysica Acta

journal homepage: www.elsevier.com/locate/bbabio

Review

FTIR studies of metal ligands, networks of hydrogen bonds, and water molecules near the active site Mn_4CaO_5 cluster in Photosystem II☆,☆☆

Richard J. Debus *

Department of Biochemistry, University of California, Riverside, Riverside, CA 92521-0129, USA

ARTICLE INFO

Article history:
Received 12 May 2014
Received in revised form 9 July 2014
Accepted 10 July 2014
Available online 16 July 2014

Keywords:
FTIR
Photosynthesis
Water oxidation
Oxygen evolving complex
Mn_4CaO_5 cluster
Hydrogen bond network

ABSTRACT

The photosynthetic conversion of water to molecular oxygen is catalyzed by the Mn_4CaO_5 cluster in Photosystem II and provides nearly our entire supply of atmospheric oxygen. The Mn_4CaO_5 cluster accumulates oxidizing equivalents in response to light-driven photochemical events within Photosystem II and then oxidizes two molecules of water to oxygen. The Mn_4CaO_5 cluster converts water to oxygen much more efficiently than any synthetic catalyst because its protein environment carefully controls the cluster's reactivity at each step in its catalytic cycle. This control is achieved by precise choreography of the proton and electron transfer reactions associated with water oxidation and by careful management of substrate (water) access and proton egress. This review describes the FTIR studies undertaken over the past two decades to identify the amino acid residues that are responsible for this control and to determine the role of each. In particular, this review describes the FTIR studies undertaken to characterize the influence of the cluster's metal ligands on its activity, to delineate the proton egress pathways that link the Mn_4CaO_5 cluster with the thylakoid lumen, and to characterize the influence of specific residues on the water molecules that serve as substrate or as participants in the networks of hydrogen bonds that make up the water access and proton egress pathways. This information will improve our understanding of water oxidation by the Mn_4CaO_5 catalyst in Photosystem II and will provide insight into the design of new generations of synthetic catalysts that convert sunlight into useful forms of storable energy. This article is part of a Special Issue entitled: Vibrational spectroscopies and bioenergetic systems.

1. Introduction

The light-driven oxidation of water in Photosystem II (PSII) produces nearly all of the O_2 on Earth and drives the production of nearly all of its biomass. Photosystem II is an integral membrane protein complex that is located in the thylakoid membranes of plants, algae, and cyanobacteria. It is a homodimer in vivo, having a total molecular weight of approximately 700 kDa with each monomer containing at least 20 different subunits and nearly 60 organic and inorganic cofactors including 35 Chl *a*, 11 carotenoid, two pheophytin, and two plastoquinone molecules. Each monomer's primary subunits include the membrane spanning polypeptides CP47 (56 kDa), CP43 (52 kDa), D2 (39 kDa), and D1 (38 kDa), and the extrinsic polypeptide PsbO (26.8 kDa). The D1 and D2 polypeptides are homologous and together form a heterodimer at the core of each monomer. Within each monomer, the CP47 and CP43 polypeptides are located on either side of the D1/D2 heterodimer and serve to transfer excitation energy from the peripherally-located antenna complex to the D1/D2 heterodimer, and specifically to the photochemically active Chl *a* multimer known as P_{680} [1–4].

The O_2-evolving catalytic center in PSII consists of a Mn_4CaO_5 cluster and its immediate protein environment. The Mn_4CaO_5 cluster accumulates four oxidizing equivalents in response to photochemical events within PSII, and then catalyzes the oxidation of two molecules of water, releasing one molecule of O_2 as a by-product [5–11]. The Mn_4CaO_5 cluster serves as the interface between single-electron photochemistry and the four-electron process of water oxidation. The photochemical events that precede water oxidation take place in the D1/D2 heterodimer. These events are initiated by the transfer of excitation energy to P_{680} following capture of light energy by the antenna complex. Excitation of P_{680} results in the formation of the charge-separated state, $P_{680}^{\bullet+}Pheo^{\bullet-}$. This light-induced separation of charge is stabilized by the rapid oxidation of $Pheo^{\bullet-}$ by Q_A, the primary plastoquinone electron acceptor, and by the rapid reduction of $P_{680}^{\bullet+}$ by Y_Z, one of two redox-active tyrosine residues in PSII. The resulting $Y_Z^{\bullet}$ in turn oxidizes the Mn_4CaO_5 cluster, while $Q_A^{\bullet-}$ reduces the secondary plastoquinone, Q_B. Subsequent charge-separations result in further oxidation of the Mn_4CaO_5 cluster and in the two-electron reduction and protonation of Q_B to form plastoquinol, which subsequently exchanges into the

☆ This article is part of a Special Issue entitled: Vibrational spectroscopies and bioenergetic systems.
☆☆ This article is dedicated to the memory of Warwick Hillier (October 18, 1967 to January 10, 2014), friend and colleague, who taught the author how to obtain FTIR spectra.
* Tel.: +1 951 827 3483; fax: +1 951 827 4294.
E-mail address: richard.debus@ucr.edu.

http://dx.doi.org/10.1016/j.bbabio.2014.07.007
0005-2728/

membrane-bound plastoquinone pool. During each catalytic cycle, two molecules of plastoquinol are produced at the Q_B site and the Mn_4CaO_5 cluster advances through five oxidation states termed S_n, where "n" denotes the number of oxidizing equivalents that are stored ($n = 0–4$). The S_1 state predominates in dark-adapted samples. The S_4 state is a transient intermediate whose formation triggers the formation and release of O_2 and the regeneration of the S_0 state.

In the recent 1.9 Å crystallographic structural model of PSII (PDB ID: 3ARC) [12,13], and in subsequent computational refinements of the structure of the Mn_4CaO_5 cluster and its ligation environment [14–19], the cluster is arranged as a distorted Mn_3CaO_4 cube that is linked to a fourth "dangling" Mn ion (denoted Mn_{A4}) by one corner oxo bridge (denoted O5) and by an additional oxygen bridging ligand (see Fig. 1). The cluster's Mn and Ca ions are ligated by six carboxylate groups and one histidine residue, all but one of which are supplied by the D1 polypeptide. Numerous immobilized water molecules are located on or near the Mn_4CaO_5 cluster, including two that are bound to Mn_{A4} (these are denoted as W1 and W2) and two that are bound to the Ca ion (these are denoted as W3 and W4). In recent proposals for the mechanism of O – O bond formation, O5 derives from one of the two substrate water molecules and becomes incorporated into the product dioxygen molecule by reacting with another substrate water-derived Mn or Ca ligand, possibly W2, W3, or a water molecule that binds to Mn_{D1} during the S_2 to S_3 transition [8,9,20–27]. Structural flexibility of the Mn_4CaO_5 cluster is a key aspect of these proposals and there is an emerging consensus that the Mn_4CaO_5 cluster readily interconverts between two nearly isoenergetic conformers during the S state cycle, with O5 ligating the dangling Mn_{A4} ion in one conformer and ligating Mn_{D1} in the other [8,9,17,19,28–32]. In the S_2 state, this interconversion is linked

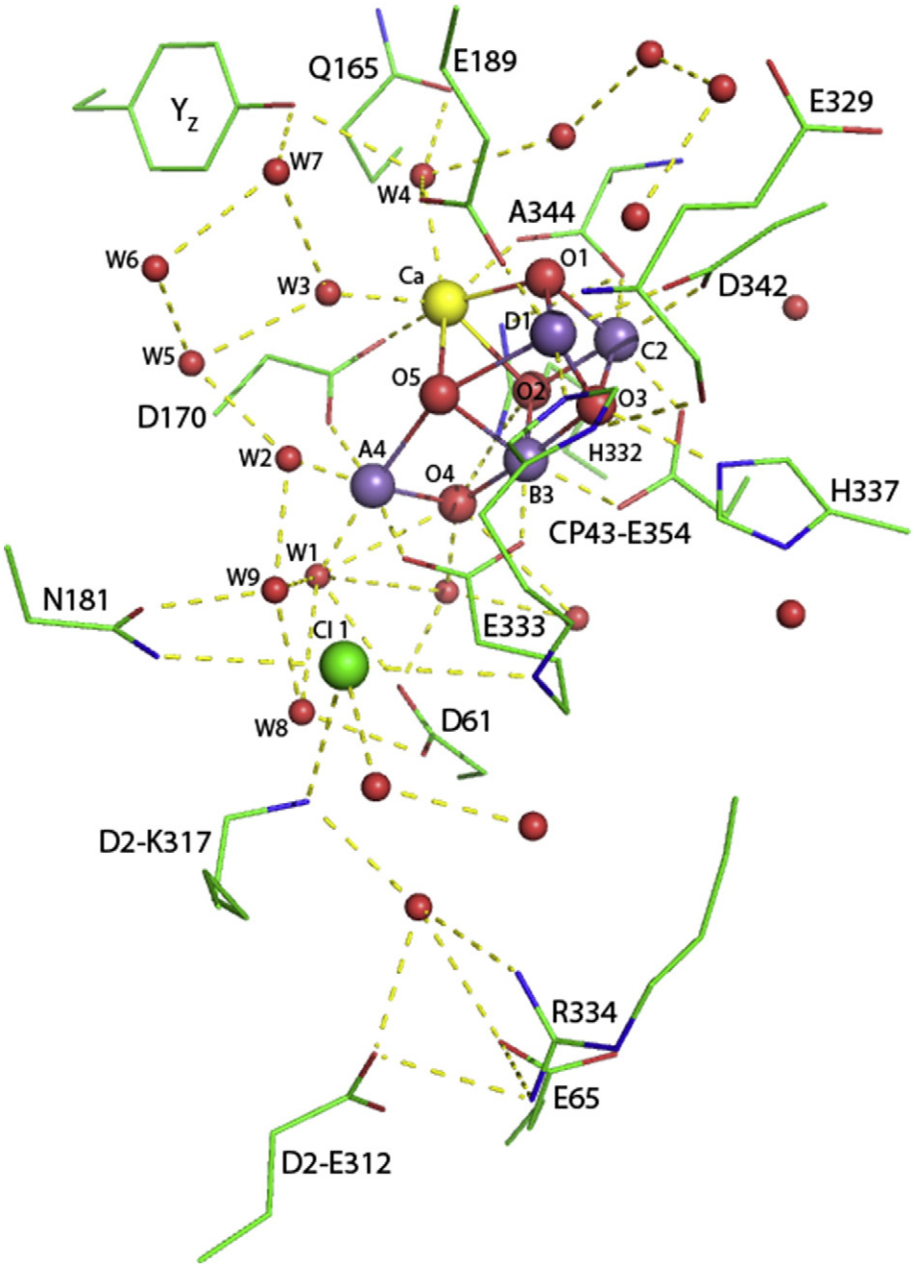

Fig. 1. The Mn_4CaO_5 cluster and its environment from the 1.9 Å structural model of PSII [12,13]. Except as noted otherwise, all residues are from the D1 polypeptide. Purple spheres, manganese ions (the labels A4, B3, C2, and D1 reflect the combined crystal structure and EPR-based notations for the Mn ions [9]); yellow sphere, calcium; green sphere, chloride; large red spheres, μ-oxo bridges; small red spheres, water molecules including the four water molecules bound to Mn_{A4} (W1 and W2) and Ca (W3 and W4). In this view, the side chain of CP43–R357 is behind μ-oxo bridge O2.

to a redox isomerization, with the Mn ion *not* binding O5 being in its Mn(III) oxidation state in addition to having an open coordination position along its Jahn–Teller axis.

Water oxidation in PSII involves a precisely choreographed sequence of proton and electron transfer steps in which the release of protons is required to prevent the redox potential of the Mn_4CaO_5 cluster from rising to levels that prevent its subsequent oxidation by $Y_Z^{\bullet}$ [33–37]. This choreography is characterized by a strictly alternating removal of electrons and protons from the Mn_4CaO_5 cluster during the S state cycle, with proton transfer preceding the oxidation of the Mn_4CaO_5 cluster during the S_2 to S_3 and S_3 to S_4 transitions [7,22,34,35,37,38]. During the S_2 to S_3 and S_3 to S_4 transitions, the trigger for proton transfer has been proposed to be the formation of $Y_Z^{\bullet}$, with the positive charge on the $Y_Z^{\bullet}$/D1-His190 pair [39] inducing the deprotonation of CP43–R357 [33,36,40,41] or a nearby cluster of water molecules [38]. In these proposals, the subsequent oxidation of the Mn_4CaO_5 cluster involves the simultaneous transfer of a proton from the Mn_4CaO_5 cluster to the now deprotonated CP43–R357 or water cluster. Experimental support for these proposals has been provided by time-resolved X-ray absorption [42,43], optical absorption [44–46], infrared absorption [47], and photothermal beam deflection [38] measurements. The measurements show that, once the $Y_Z^{\bullet}S_3$ state is achieved, electron transfer from the Mn_4CaO_5 cluster to $Y_Z^{\bullet}$ (with concomitant O_2 formation) takes place only after a lag of 200–250 μs that is assigned to the time for proton removal. The deprotonation of CP43–R357 (or the cluster of water molecules) is envisioned to take place via one or more proton egress pathways leading from the Mn_4CaO_5 cluster to the thylakoid lumen. These pathways are expected to be comprised of networks of hydrogen bonds involving protonatable amino acid side chains and water molecules. Several possible pathways for water access, O_2 egress, and proton egress have been identified in the 1.9 Å [12,13] and earlier 3.5 Å to 2.9 Å [48–50] crystallographic structural models on the basis of visual examinations [12,48,51–54], electrostatic calculations [55], solvent accessibility simulations [56], cavity searching algorithms [50,57,58], molecular dynamics simulations of water diffusion [59–62], and the identification of oxidatively-modified amino acid residues in the interior of PSII [63,64] (for review, see Refs. [54,65–67]).

FTIR difference spectroscopy is an extremely sensitive tool for characterizing the dynamic structural changes that occur during an enzyme's catalytic cycle [68–72]. It is particularly well suited for analyzing polypeptide conformational changes, protonation/deprotonation reactions of amino acid side chains, and the structural changes of hydrogen bonded water molecules. In PSII, the frequencies of numerous vibrational modes change as the Mn_4CaO_5 cluster is oxidized through the S state cycle, including many modes that are attributable to carboxylate residues and hydrogen-bonded water molecules [73–76]. This review focuses on the studies designed to characterize the structural changes of the Mn_4CaO_5 cluster's protein ligands that may occur during the individual steps in the catalytic cycle, to delineate the networks of hydrogen bonds that form the dominant proton egress pathways leading from the Mn_4CaO_5 cluster to the thylakoid lumen, and to determine the influence of specific amino acid residues on the water molecules located on or near the Mn_4CaO_5 cluster, some of which may serve as substrate for O_2 formation. Another review in this issue focuses on other aspects of the electron and proton transfer reactions that accompany the oxidation of water to dioxygen in PSII, including dynamic aspects [77].

2. Metal ligation

2.1. Mid-frequency region

Mid-frequency S_2-*minus*-S_1 FTIR difference spectra of PSII core complexes free of contributions from the quinone electron acceptors were first reported between 1992 and 1999 [78–83]. The first mid-frequency S_3-*minus*-S_2 FTIR difference spectrum was reported in 2000 [84]. The first sets of complete mid-frequency S_{n+1}-*minus*-S_n FTIR difference spectra were reported in two back-to-back publications in 2001 [85,86]. The importance of sample hydration for observing these spectra was pointed out in 2002 [87]. The individual S_{n+1}-*minus*-S_n FTIR difference spectra of wild-type PSII core complexes contain a wealth of spectral features (e.g., Fig. 2). On the basis of their downshifts in samples that had been globally labeled with ^{13}C or ^{15}N, features appearing between 1700 and 1630 cm^{-1} were assigned to amide I modes, some features appearing between 1600 and 1500 cm^{-1} were assigned to amide II modes and others to asymmetric carboxylate stretching [$\nu_{asym}(COO^-)$] modes, and features appearing between 1450 and 1300 cm^{-1} were assigned to symmetric carboxylate stretching [$\nu_{sym}(COO^-)$] modes [88–91]. On the basis of a 7 cm^{-1} downshift in samples that had been specifically labeled with ^{15}N-histidine, a negative feature near 1113–1114 cm^{-1} in the S_2-*minus*-S_1 FTIR difference spectrum was assigned to the C–N stretching mode of a histidyl imidazole ring whose π nitrogen is protonated, with the Nπ–H group participating in a hydrogen bond [83]. The appearance of the 1113–1114 cm^{-1} feature in the S_2-*minus*-S_1 spectrum was taken to imply that the τ nitrogen of this histidine (now presumed to be D1-H332) ligates a Mn ion [83]. Subsequent work showed that this spectral feature is positive in the S_1-*minus*-S_0 spectrum, negative in the S_2-*minus*-S_1 and S_3-*minus*-S_2 spectra, and absent from the S_0-*minus*-S_3 spectrum [92]. It was concluded that changes to the vibrational mode that occur during the S_0 to S_1 transition are reversed during the S_1 to S_2 and S_2 to S_3 transitions and that the mode is not perturbed during the S_3 to S_0 transition [92].

2.1.1. The C-terminus of the D1 polypeptide at Ala344

Attempts to assign features in the S_{n+1}-*minus*-S_n difference spectra to individual amino acid residues began appearing in 2004. To test the proposal [93] that the C-terminus of the D1 polypeptide at D1-A344 ligates one or more Mn ions, the mid-frequency FTIR difference spectra of unlabeled and L-[1-^{13}C]alanine-labeled wild-type *Synechocystis* PSII core complexes were compared. Two independent FTIR studies showed that the incorporation of L-[1-^{13}C]alanine altered the wild-type S_2-*minus*-S_1 mid-frequency FTIR difference spectrum in the symmetric carboxylate stretching region [94,95]. The ^{12}C-*minus*-^{13}C double difference spectrum of this region (Fig. 3) showed that the alterations represent the ^{13}C-induced shift of a single vibrational mode. In the S_1 state, this mode appears at ~1355 cm^{-1} and is shifted by ^{13}C to either ~1339 or ~1320 cm^{-1}. In the S_2 state, this mode appears at either ~1339 or ~1320 cm^{-1} and is shifted by ^{13}C to ~1302 cm^{-1}. This mode could be assigned unambiguously to the α-COO^- group of Ala344 because the mode was *not* shifted by the incorporation of L-[1-^{13}C]alanine into either D1-A344G or D1-A344S PSII core complexes (Fig. 3) [94,95] (the C-terminal α-COO^- group of the D1 polypeptide cannot be labeled in either mutant because it is not provided by alanine). On the basis of the observed frequencies, it was concluded that the α-COO^- group of D1-A344 is a unidentate ligand of a metal ion in both S_1 and S_2 states [94,95]. The mode downshifts by ~17 cm^{-1} or ~36 cm^{-1} during the S_1 to S_2 transition [94,95] and is restored during the S_3 to S_0 transition [95,96]. These frequency shifts were taken to imply that the ligating C–O bond weakens during the S_1 to S_2 transition and is restored during the S_3 to S_0 transition. This weakening was attributed to the increased charge that develops on the Mn_4CaO_5 cluster during the S_1 to S_2 transition. Consequently, it was proposed that the α-COO^- group of Ala344 ligates a Mn ion whose charge or formal oxidation state increases during the S_1 to S_2 transition [94,95,97]. However, on the basis of QM/MM analyses performed in conjunction with the earlier ~3.5 Å crystallographic structural model [48], it was concluded that the partial atomic charges of the individual Mn ions would change little during any of the S state transitions, and that a redistribution of charge on the Mn_4CaO_5 cluster during the S_1 to S_2 transition could produce a similar downshift if D1-

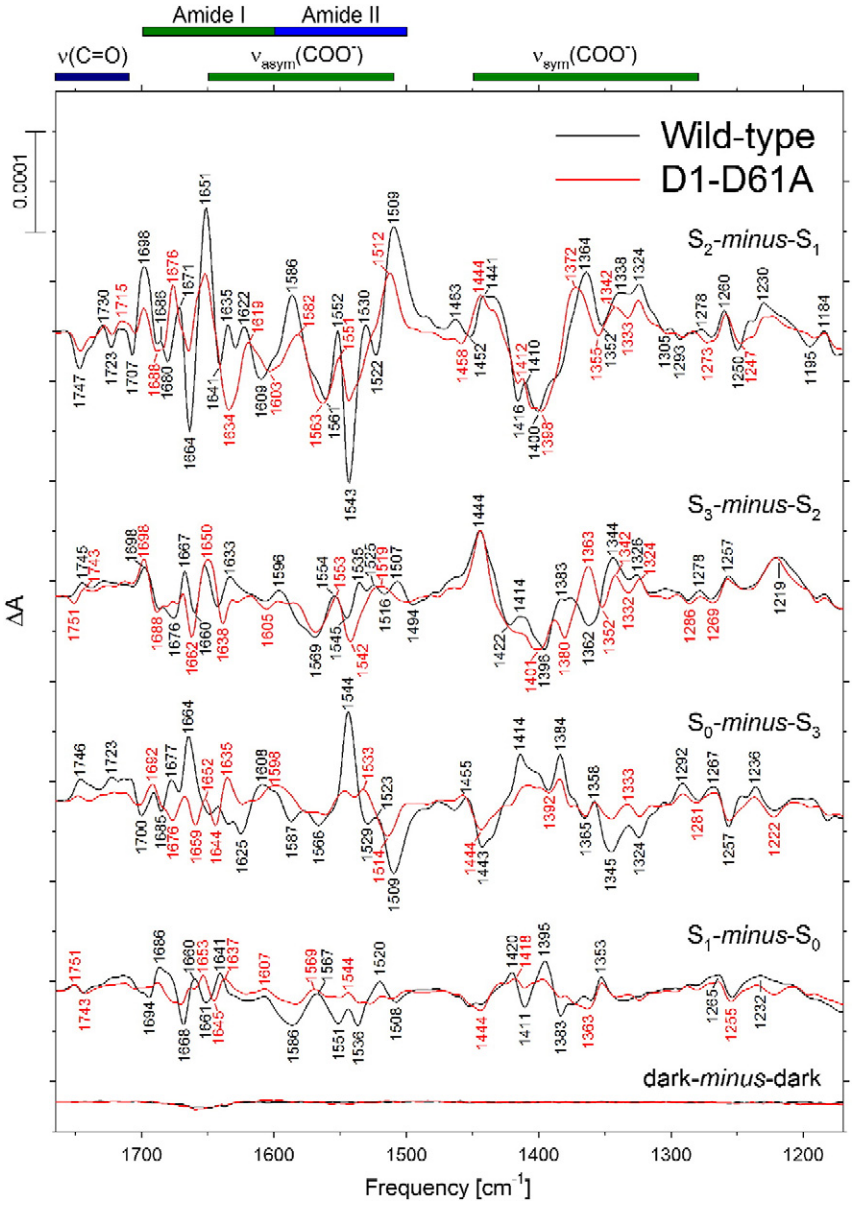

Fig. 2. Comparison of the mid-frequency FTIR difference spectra of wild-type (black) and D1-D61A (red) PSII core complexes in response to four successive flash illuminations applied at 0 °C. The "S_0-*minus*-S_3" and "S_1-*minus*-S_0" spectra of D1-D61A probably correspond to a mixture of S state transitions . Dark-*minus*-dark control traces are included to show the noise level (lower traces).
Reprinted with permission from Ref. [126]. Copyright 2014, American Chemical Society.

A344 was coordinated to the Ca ion [36,98,99]. Indeed, the α-COO^- group of Ala344 forms an asymmetric bridge between the Ca ion and Mn_{C2} in the 1.9 Å crystallographic structural model [12,13] (Fig. 1). Furthermore, most of the other carboxylate ligands of the Mn_4CaO_5 cluster are insensitive to the oxidations of the cluster that occur during the S state cycle (see below, Section 2.1.3). Consequently, the reason that the $\nu_{sym}(COO^-)$ mode of D1-A344 downshifts during the S_1 to S_2 transition is not known. Perhaps the reason is related to one conclusion of a polarized attenuated total reflection FTIR study [100], that D1-Ala344 may significantly change its orientation during the S_1 to S_2 transition.

2.1.2. CP43–Glu354

The S_2-*minus*-S_1 FTIR difference spectrum of CP43–E354Q PSII core complexes shows alterations throughout the amide II, $\nu_{asym}(COO^-)$ and $\nu_{sym}(COO^-)$ regions [101–103]. Global labeling with ^{15}N showed that the CP43–E354Q mutation perturbs both amide II and carboxylate stretching modes [103]. Specific labeling with L-[1-^{13}C]alanine showed that the CP43–E354Q mutation shifts the $\nu_{sym}(COO^-)$ mode of the α-COO^- group of D1-Ala344 to higher frequencies by 3–6 cm^{-1} in both S_1 and S_2 states [103]. These data show that the CP43–E354Q mutation perturbs multiple carboxylate groups in the vicinity of the Mn_4CaO_5 cluster. In one study [102], negative features at 1525 cm^{-1} and 1394 cm^{-1} in the S_2-*minus*-S_1 FTIR difference spectrum of wild-type PSII were assigned to the $\nu_{asym}(COO^-)$ and $\nu_{sym}(COO^-)$ modes of CP43–E354 in the S_1 state, respectively, and the positive features at 1502 cm^{-1} and 1431 cm^{-1} were assigned to the $\nu_{asym}(COO^-)$ and $\nu_{sym}(COO^-)$ modes of CP43–E354 in the S_2 state, respectively [102]. On the basis of these assignments, CP43–E354 was proposed to bridge two Mn ions in the S_1 state and shift to chelating bidentate coordination of a single Mn ion in the S_2 state [102]. However, in another study [103], the positive feature near 1502 cm^{-1} was assigned to an amide II mode on the basis of its downshift by 14–15 cm^{-1} after global labeling with ^{15}N (although the presence of the $\nu_{asym}(COO^-)$ mode at the same frequency could not be excluded

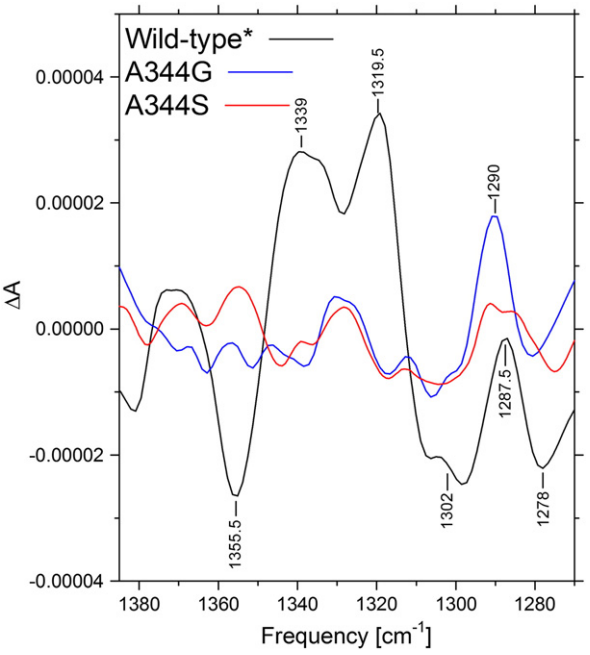

Fig. 3. Comparison of the double difference spectra, ^{12}C-*minus*-^{13}C, of wild-type (black), D1-A344G (blue) and D1-A344S (red) PSII core complexes obtained by subtracting the S_2-*minus*-S_1 FTIR difference spectra of [1-^{13}C]alanine-labeled samples from the S_2-*minus*-S_1 FTIR difference spectra of unlabeled samples.
Reprinted with permission from Ref. [94]. Copyright 2004, American Chemical Society.

because of the feature's breadth). In agreement with Ref. [102], this study assigned a negative feature at 1524 cm^{-1} to the $\nu_{asym}(COO^-)$ mode of CP43–E354 in the S_1 state and concluded that CP43–E354 serves a as a bridging ligand between two Mn ions in the S_1 state [103]. However, this study was unable to confirm that the coordination mode of CP43–E354 changes during the S_1 to S_2 transition because the $\nu_{sym}(COO^-)$ mode of CP354 could not be identified unambiguously. In this study, CP43–E354Q PSII core complexes were found to have an unusually stable S_2 state and to be heterogeneous, with most PSII reaction centers unable to advance beyond the S_3 state, but with some (approximately 20% of the total) able to advance through the S state transitions with normal S state parameters [103]. In a subsequent polarized attenuated total reflection FTIR study, it was concluded that CP43–E354 changes its orientation by ~8° during the S_1 to S_2 transition [100]. This reorientation would be consistent with changing from bridging to chelating coordination [100]. The S_3-*minus*-S_2 FTIR difference spectrum was unaltered by the CP43–E354Q mutation [102], showing that the protein's response to the changes in the Mn_4CaO_5 cluster's geometry that occur during the S_2 to S_3 transition is not changed by the mutation.

2.1.3. D1-Asp170, D1-Glu189, D1-Glu333, and D1-Asp342

The mutations D1-D170H [104,105], D1-E189Q [106,107], D1-E189R [107], D1-E333Q [108], and D1-D342N [109] produced no significant changes in any of the S_{n+1}-*minus*-S_n FTIR difference spectra; that is, they produced no changes greater than those caused by mutations created far from the Mn_4CaO_5 cluster (e.g., D2-H189Q, near Y_D) or by differences in handling wild-type samples [107]. In particular, none of these mutations eliminated any carboxylate stretching modes and none produced any significant changes in polypeptide backbone conformations as shown by a lack of significant mutation-induced alterations to the amide I and amide II regions of the spectra.[1] This result was entirely unexpected. It had long been assumed that most of the features in the S_{n+1}-*minus*-S_n FTIR difference spectra would correspond to the Mn_4CaO_5 cluster's amino acid ligands. Indeed, one of the most striking results of the FTIR studies on PSII is that the individual FTIR difference spectra are insensitive to the individual mutation of four of the Mn_4CaO_5 cluster's six carboxylate ligands. Evidently, most of the features in the mid-frequency S_{n+1}-*minus*-S_n FTIR difference spectra correspond to residues in the cluster's second coordination sphere or beyond and reflect the broad response of the protein to the electrostatic influences that arise from the positive charge that develops on the Mn_4CaO_5 cluster during the S_1 to S_2 transition [44,111–120] and to the structural changes that are associated with the S_2 to S_3, S_3 to S_0, and S_0 to S_1 transitions [31,121–123]. Indeed, mutations of residues located 5–11 Å from the nearest Mn ion and thought to participate in proton egress pathways cause the greatest changes in the S_{n+1}-*minus*-S_n FTIR difference spectra [124–126] (e.g., see Fig. 2 and see below, Section 3.2). The simplest explanation for the insensitivity of the S_2-*minus*-S_1 FTIR difference spectrum to the individual mutation of most the cluster's carboxylate ligands is that the positive charge that develops on the Mn_4CaO_5 cluster during the S_1 to S_2 transition is highly delocalized at ambient temperatures. There is precedent for such delocalization in mixed-valence inorganic metal complexes [127–129]. Furthermore, comparative resonant inelastic X-ray scattering (RIXS) studies of Mn oxides, Mn coordination complexes, and spinach PSII membranes have provided strong evidence that the oxidations of the Mn_4CaO_5 cluster that occur during the S state transitions involve electrons that are strongly delocalized throughout the cluster and may involve the cluster's ligands [130,131]. Delocalization would also be consistent with the conclusions of the QM/MM analyses mentioned above [36,98,99]. Consequently, the reason that one or more carboxylate stretching modes of D1-A344 [94,95,97] and CP43–E354 [102,103] shift during the S_1 to S_2 transition may be that the carboxylate group of the former changes its orientation and the carboxylate group of the latter changes its coordination mode during this transition.

2.2. Low frequency region

Vibrations of the Mn_4CaO_5 cluster's core and of its metal-ligand bonds appear between 650 and 350 cm^{-1}. The first S_2-*minus*-S_1 FTIR difference spectrum of this region appeared in 2000 [132], the first S_3-*minus*-S_2 difference spectrum of this region appeared in 2001 [133], and the first set of complete S_{n+1}-*minus*-S_n difference spectra in this region appeared in 2005 [134]. In the S_2-*minus*-S_1 difference spectrum, a positive band at 606 cm^{-1} and a negative band at 625 cm^{-1} downshifted ~10 cm^{-1} in samples that had been exchanged into $H_2^{18}O$ but were unaffected by replacing ^{40}Ca with ^{44}Ca [132]. On the basis of these observations and comparisons with model compounds, the bands were assigned to a Mn–O–Mn cluster mode in a multiply bridged structure that might include additional oxo or carboxylate bridges [132,135]. Many of the bands in the low-frequency S_2-*minus*-S_1 difference spectrum, including the 606 cm^{-1} band, were shifted by global labeling with ^{13}C and/or ^{15}N [90]. These bands were proposed to include vibrational modes of bonds between Mn ions and carbon-containing or nitrogen-containing groups (e.g., Mn–COO^- bending modes). A negative band at 577 cm^{-1} was shifted by neither ^{13}C nor ^{15}N (nor ^{18}O [132]) and was attributed a skeletal vibration of the Mn_4CaO_5 cluster or to a Mn–O vibrational mode involving a non-^{18}O-exchangeable oxygen atom [90]. The 606 cm^{-1} band in the S_2 state appeared to change sign and intensity during the S state cycle [134], implying S state-dependent changes in the core structure of the Mn_4CaO_5 cluster. Other prominent bands between 638 and 594 cm^{-1} also changed sign and intensity during the S state cycle [134]. Some of these were also assigned to Mn_4CaO_5 cluster modes on the basis of their sensitivity to $H_2^{18}O$ substitution and insensitivity to D_2O substitution [134]. Other low-frequency bands were sensitive to D_2O substitution, but were insensitive to $H_2^{18}O$ substitution [134]. These

[1] There is a report that the D1-D170E mutation causes spectral alterations consistent with a change in carboxylate coordination to Mn or Ca during the S_1 to S_2 transition [110], but the wild-type control spectrum in this study is unlike that observed by any other laboratory and is undoubtedly dominated by artifacts (see Footnote 2 of Ref. [94]).

were assigned to modes from amino acid side chains and polypeptide backbones associated with exchangeable hydrogen in hydrophilic environments [134]. Still other bands were sensitive to both $H_2^{18}O$ and D_2O exchange and were attributed to Mn – O and/or Mn – OH_2 stretching modes, to wagging modes of Mn-bound water molecules, or possibly to Ca – OH and/or Ca – OH_2 modes [134].

The 606 cm^{-1} band in the S_2 state shifts to ~618 cm^{-1} when Ca is replaced with Sr [132,135,136], shifts to ~613 cm^{-1} in the mutants D1-D170H [104] and D1-A344G [137], and shifts to ~623 cm^{-1} in the mutant D1-E189Q [106]. These observations show that D1-D170 and D1-E189 are coupled structurally to the Mn_4CaO_5 cluster, despite the absence of changes in the mid-frequency region produced by the mutations D1-D170H [104,105] and D1-E189Q [106,107]. Other features in the 640 to 570 cm^{-1} region were also perturbed by the mutations D1-D170H [104], D1-A344G [137], and D1-E189Q [106]. In particular, a negative band near 617 cm^{-1} appears diminished by all three mutations. The latter feature was also diminished slightly when D1-Ala344 was specifically labeled with ^{13}C [95]. Recently, the 606 cm^{-1} mode in the S_2 state was shown to be eliminated or shifted to 623 cm^{-1} by ammonia [138]. Ammonia has been proposed to either exchange into an oxo bridge [138,139] (proposed to be O5 [10,75,138]), or to exchange for W1 on Mn_{A4} [26,27,140] (see competing discussions in Refs. [26,27,140] versus [10]). The mutations and treatments that alter the 606 cm^{-1} band all have been directed at the face of the Mn_4CaO_5 that includes the Ca ion, Mn_{A4}, Mn_{D1}, and O_5. It would be of interest to examine the low-frequency FTIR difference spectra of mutations constructed at D1-E333, D1-D342, and CP43–E354 to see if the 606 cm^{-1} feature is altered by mutations on the other "side" of the Mn_4CaO_5 cluster.

3. Networks of hydrogen bonds

3.1. Arginine

In recent proposals, the oxidation of the Mn_4CaO_5 cluster during the S_2 to S_3 and S_3 to S_4 transitions involves the simultaneous transfer of a proton from the Mn_4CaO_5 cluster to a deprotonated CP43–R357 or a deprotonated water cluster. To test whether CP47–Arg357 is coupled structurally with the Mn_4CaO_4 cluster, a strain of *Synechocystis* sp. PCC 6803 was engineered to be deficient in arginine biosynthesis and cells were propagated in the presence of [$\eta_{1,2}$-$^{15}N_2$]Arg or [ζ-^{13}C]Arg [141]. The S_2-*minus*-S_1 FTIR difference spectra of [$\eta_{1,2}$-$^{15}N_2$]Arg-labeled PSII core complexes showed Arg-attributable bands between 1700 and 1600 cm^{-1}. The S_2-*minus*-S_1 FTIR difference spectra of [ζ-^{13}C]Arg-labeled PSII core complexes showed Arg-attributable bands between 1700 and 1550 cm^{-1}. These bands were assigned to the CN/NH_2 vibrations of a guanidinium group [141]. Their frequencies are similar to those of ^{15}N-labeled and ^{13}C-labeled arginine in aqueous solution. These observations provide spectroscopic evidence that the fully protonated guanidinium group of an arginine residue (presumed to be CP43–R357, the only Arg residue within 10 Å of the Mn_4CaO_5 cluster) is coupled structurally with the Mn_4CaO_5 cluster, presumably by participating in hydrogen bonds with ligands of Mn or Ca [141]. A direct interaction between CP43–R357 and the first coordination shell of the Mn_4CaO_5 cluster was confirmed by the 1.9 Å crystallographic structural model [12,13]. In this model, one of the η nitrogen atoms of the guanidino group of CP43–Arg357 forms a hydrogen bond to each of the Mn_4CaO_5 cluster's O2 and O4 oxo bridges and the other η nitrogen atom form hydrogen bonds with the carboxylate groups of D1-D170 and D1-A344. Mims ENDOR experiments performed with [$\eta_{1,2}$-$^{15}N_2$] Arg-labeled PSII core complexes purified from an independently constructed strain of *Synechocystis* showed the presence of ^{15}N couplings to the S_2 state of the Mn_4CaO_5 cluster, providing addition evidence of structural coupling between the guanidinium group of an Arg residue (also presumed to be CP43–R357) and the Mn_4CaO_5 cluster (P. Oyala, R J. Debus, and R. D Britt, unpublished).

3.2. The carbonyl stretching modes of carboxylic acids

The region between 1790 and 1710 cm^{-1} contains the carbonyl stretching [ν(C═O)] modes of protonated carboxylate residues [70,71,142] as well as the keto and ester C═O vibrations of chlorophyll, pheophytin, heme, and lipids [143]. Deuteration helps distinguish between these modes because it removes the weak coupling that exists between the C═O stretching and C – O – H bending modes of the COOH group. The elimination of this coupling causes the ν(C═O) mode to downshift by 4–20 cm^{-1} [142,144–147]. This D_2O-induced downshift is diagnostic for the ν(C═O) mode of protonated carboxylate residues and has been used as such in many systems, including bacteriorhodopsin [144,148–151], rhodopsin [152,153], bacterial reaction centers [154–157], heme-copper oxidases [158–161] and photoactive yellow protein [162]. In PSII core complexes from *Synechocystis* sp. PCC 6803, a negative feature is observed at ~1747 cm^{-1} in the S_2-*minus*-S_1 difference spectrum, a positive feature is observed at ~1745 cm^{-1} in the S_3-*minus*-S_2 difference spectrum, a positive feature is observed at ~1746 cm^{-1} in the S_0-*minus*-S_3 difference spectrum, and a derivative-shaped feature is observed at ~1751(+)/1744(−) cm^{-1} in the S_1-*minus*-S_0 difference spectrum [124,125]. These features downshift 4–7 cm^{-1} after exchange into buffers containing D_2O [124,125] (see Fig. 4). On the basis of these downshifts, it was concluded that these features correspond to the ν(C═O) modes of protonated carboxylate groups [124,125]. The frequency of the ν(C═O) mode of a carboxylic acid residue depends on the number and strengths of hydrogen bonds involving its C═O and O – H moieties [142,144–147]. Their frequencies in the S_{n+1}-*minus*-S_n FTIR difference spectra suggest that each of the protonated carboxylate groups giving rise to these features participates in a single hydrogen bond that involves the C═O moiety [146,147], although participation in two hydrogen bonds, with one involving the oxygen of the C – O – H group [147], could not be excluded.

3.2.1. Network of hydrogen bonds extending at least 20 Å

The negative feature at ~1747 cm^{-1} in the S_2-*minus*-S_1 spectrum of PSII core complexes from *Synechocystis* sp. PCC 6803 has been proposed to correspond to a carboxylate group whose pK_a value decreases in response to the increased charge that develops on the Mn_4CaO_5 cluster during the S_1 to S_2 transition [124,125]. It was proposed that (i) the structural response of PSII to the charge that develops on the Mn_4CaO_5 cluster during this transition is transmitted electrostatically and through networks of hydrogen bonds, and (ii) this structural response alters the environment of the carboxylate group responsible for the ~1747 cm^{-1} feature, causing its pK_a value to decrease [124,125]. This feature is eliminated by the mutations D1-E65A, D2-E312A, and D1-E329Q [124], is diminished substantially by the mutations D1-D61A [126] and D1-R334A [125], and is diminished or eliminated by the over-dehydration of samples [124] (see Fig. 5). Consequently, it was proposed that (i) D1-D61, D1-E65, D1-E329, D1-R334, and D2-E312 participate in the same network of hydrogen bonds as the unidentified carboxylate group responsible for the negative ~1747 cm^{-1} feature and (ii) the mutation of any of these residues to a non-protonatable residue, or the over dehydration of samples, disrupts the network sufficiently that the structural perturbations associated with S_1 to S_2 transition are either transmitted to the unidentified carboxylate less efficiently or not at all, thereby diminishing or eliminating the ~1747 cm^{-1} feature [124,125]. Because D1-E329 is located over 20 Å from the D1-D61 and the interacting D1-E65/D2-E312/D1-R334 triad, this network of hydrogen bonds must extend at least 20 Å across the lumenal face of the Mn_4CaO_5 cluster (see Figs. 1 and 6). It is an open question whether elements of the proposed network exist only transiently like the networks of hydrogen bonds that transiently connect hydrophilic pockets in a recent molecular dynamics study [59].

The unidentified carboxylate group that corresponds to the negative ~1747 cm^{-1} feature could be the side chain of D1-E65, D2-E312, or D1-

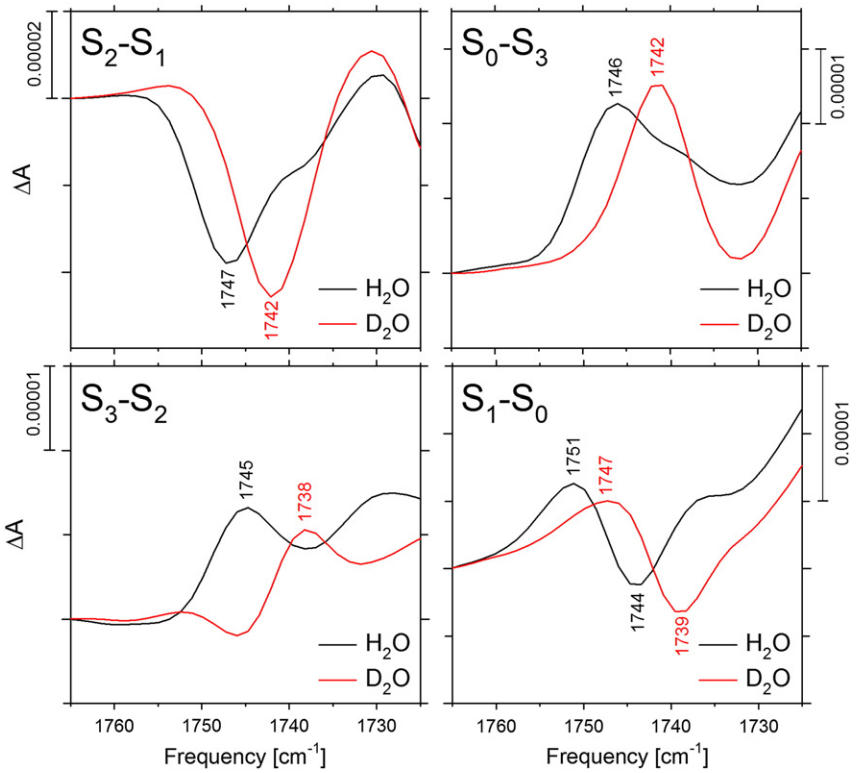

Fig. 4. Comparison of the protonated carboxylic acid carbonyl stretching regions of wild-type PSII core complexes in the presence of H_2O and D_2O. Note the different vertical scales.

E329 or another carboxylate residue located in the same proposed network of hydrogen bonds. It is not D1-D61 because the D1-D61A mutation does not eliminate the feature. Some constraints on the location of the unidentified carboxylate residue are provided by the observation that the feature is unaltered by the D1-Q165E, D2-E307Q, D2-D308N, D2-E310Q, and D2-E323Q mutations [125]. Because D1-Q165 is located across the Mn_4CaO_5 cluster from D1-D61 and the D1-E65/D2-E312/D1-R334 triad, and because D2-E307, D2-D308, D2-E310, and D2-E323 lie even farther from the Mn_4CaO_5 cluster (see Fig. 6), it was concluded that the unidentified carboxylate residue must be D1-E65, D2-E312, a residue in their vicinity, or a residue between the D1-E65/D2-E312/D1-R334 triad and D1-E329. The residue D1-D59 was suggested as one possibility [125]. The closest distance between the carboxylate oxygens of this residue and those of D1-E65 is 6.9 Å.

3.2.2. Network of hydrogen bonds extending at least 13 Å

The positive feature at ~1745 cm^{-1} in the S_3-*minus*-S_2 FTIR difference spectrum of PSII core complexes from *Synechocystis* sp. PCC 6803 was proposed to correspond to a *second* carboxylic acid group, one whose pK_a value *increases* during the S_2 to S_3 transition [125]. The structural response of PSII to the geometric changes in the Mn_4CaO_5 cluster that accompany this transition [31,121–123] was presumed to be transmitted through networks of hydrogen bonds, altering the environment of the unidentified carboxylate group responsible for the positive ~1745 cm^{-1} feature, causing its pK_a value to increase. The ~1745 cm^{-1} feature was eliminated by the mutations D1-E329Q [124] and D1-Q165E [125]. Consequently, it was proposed that D1-E329 and D1-Q165 participate in the same network of hydrogen bonds as the unidentified carboxylate group responsible for the positive ~1745 cm^{-1} feature and that the mutation of either of these residues disrupts the network sufficiently that the structural perturbations associated with S_2 to S_3 transition are no longer transmitted to the unidentified carboxylate, thereby eliminating the ~1745 cm^{-1} feature [125]. Although the D1-Q165E mutation eliminates the ~1745 cm^{-1} feature from the S_3-*minus*-S_2 difference spectrum, it has no effect on the ~1747 cm^{-1} feature in the S_2-*minus*-S_1 difference spectrum [125]. The mutation's disparate effect on the ~1747 and ~1745 cm^{-1} features was taken to provide a constraint on the identity of this second carboxylate residue: it must be located closer to D1-Q165 than to the D1-E65/D2-E312/D1-R334 triad. One possibility is D1-E329. The mutation D1-E329Q would then eliminate the positive ~1745 cm^{-1} feature from the S_3-*minus*-S_2 spectrum directly and eliminate the negative ~1747 cm^{-1} feature from the S_2-*minus*-S_1 spectrum by disrupting the network of hydrogen bonds discussed in Section 3.2.1. Because the side chain of D1-E329 is located approximately 13 Å from the side chain of D1-Q165, this network must extend at least 13 Å across face of the Mn_4CaO_5 cluster opposite from the D1-E65/D2-E312/D1-R334 triad (see Figs. 1 and 6). Because D1-E329 also participates in a network of hydrogen bonds that includes D1-D61 and the D1-E65/D2-E312/D1-R334 triad (see Section 3.2.1), the overall network must be quite extensive. Indeed, the ~1745 cm^{-1} feature in the S_3-*minus*-S_2 difference spectrum is altered by the D1-D61A mutation [126], showing that D1-D61 participates in a network of hydrogen bonds extending to D1-Q165. The participation of D1-Q165 in such an extensive network of hydrogen bonds is expected on the basis of the 1.9 Å structural model [12,13] and is supported by a recent QM/MM study [163]. In the 1.9 Å structural model, W4 forms hydrogen bonds with both D1-Q165 and the phenolic oxygen of Y_Z (D1-Y161) and participates in an extensive network of hydrogen bonds that extends across the Mn_4CaO_5 cluster and via the Cl^- (1) ion and D2-K317 to the lumenal surface. This network includes D1-E189 and several water molecules including W3, the other water ligand of the Ca ion, and W2, one of two water ligands of the dangling Mn_{A4} ion. A possible role for D1-Q165 in a channel consisting of an extensive network of hydrogen bonds had been suggested on the basis of analyses conducted before the 1.9 Å structural model became available [50,56,58]. As noted previously, it is an open question whether elements of the proposed networks exist only transiently.

The pK_a shifts giving rise to the negative ~1747 cm^{-1} feature in the S_2-*minus*-S_1 difference spectrum and the positive ~1745 cm^{-1} feature in the S_3-*minus*-S_2 difference spectrum appear to be reversed during

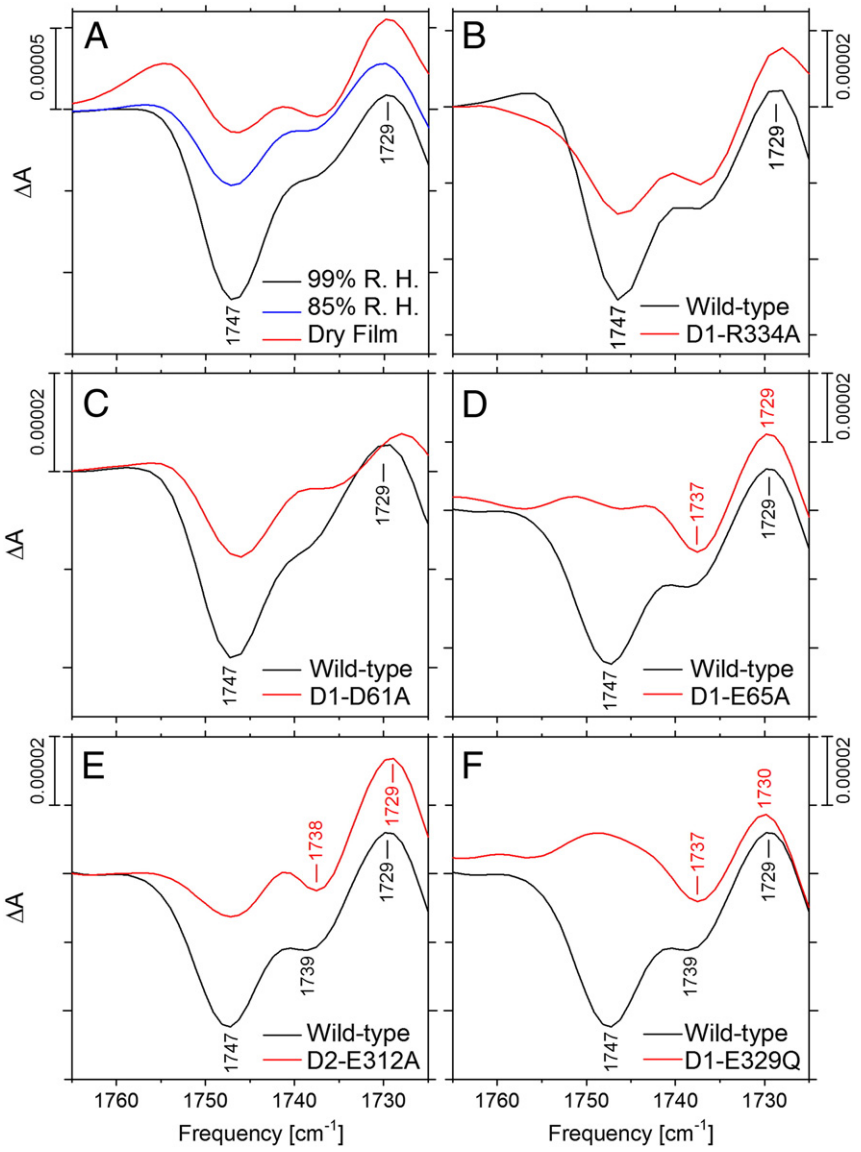

Fig. 5. Comparison of the protonated carboxylic acid carbonyl stretching regions of (A) wild-type PSII core complexes maintained at a relative humidity of 99% (black) or 85% (blue) or as a dry film in the sample cell (red), (B) wild-type (black) and D1-R334A (red) PSII core complexes, (C) wild-type (black) and D1-D61A (red) PSII core complexes, (D) wild-type (black) and D1-E65A (red) PSII core complexes, (E) wild-type (black) and D1-E312A (red) PSII core complexes, and (F) wild-type (black) and D1-E329Q (red) PSII core complexes.

the S_3 to S_0 transition, with the positive amplitude of the ~1746 cm^{-1} feature in the S_0-*minus*-S_3 FTIR difference spectrum reflecting the larger amplitude of the negative ~1747 cm^{-1} feature in the S_2-*minus*-S_1 difference spectrum compared to the positive ~1745 cm^{-1} feature in the S_3-*minus*-S_2 difference spectrum (Fig. 4) [125]. The derivative nature of the ~1751(+)/1744(−) cm^{-1} feature in the S_1-*minus*-S_0 spectrum was proposed to reflect a change in the environment of a third carboxylic acid group during the S_0 to S_1 transition that does not change this group's pK_a value. Although this environmental change would be expected to reverse during the other S state transitions, the amplitude of this feature is sufficiently weak that any such reversal is probably lost beneath the larger ~1747 and ~1745 cm^{-1} features in the other S_{n+1}-*minus*-S_n FTIR difference spectra.

The features at 1747 and 1745 cm^{-1} discussed in the preceding paragraphs have not been observed in PSII core complexes from *Thermosynechococcus elongatus* [85,87,89,164–166], PSII membranes from spinach [79,80,86,136], or in some preparations of PSII core complexes from *Synechocystis* sp. PCC 6803 [95,102,104,106,137]. Their absence in *T. elongatus* and spinach might derive from the slight differences between the amino acid sequences of the PSII polypeptides in different organisms. However, the observation of these features may depend on preparation. In any case, we have observed these features under a variety of conditions in *Synechocystis* sp. PCC 6803 [103,105,107–109,124–126,167]. The sensitivity of these features to the extent of sample hydration and to the mutation of selected single amino acid residues shows the sensitivity of the corresponding carboxylate groups to minor changes in protein environment.

3.2.3. A dominant proton egress pathway

The kinetically efficient transfer of protons through a potential channel requires finely tuned pK_a differences between key residues and the transient formation of clusters of water molecules [168–171]. Consequently, mutation of key residues in a dominant proton egress pathway would be expected to slow oxidation of the Mn_4CaO_5 cluster in the same manner that mutations that impair proton uptake slow electron transfer from $Q_A^{\bullet-}$ to $Q_B^{\bullet-}$ in reaction centers of *Rhodobacter sphaeroides* [172–174] and the reduction of O_2 to H_2O in cytochrome *c* oxidase [175–177]. A network of hydrogen bonds leading from the Mn_4CaO_5 cluster to the thylakoid lumen via D1-D61 and the D1-E65/D2-E312/D1-R334 triad can been inferred from the distribution of

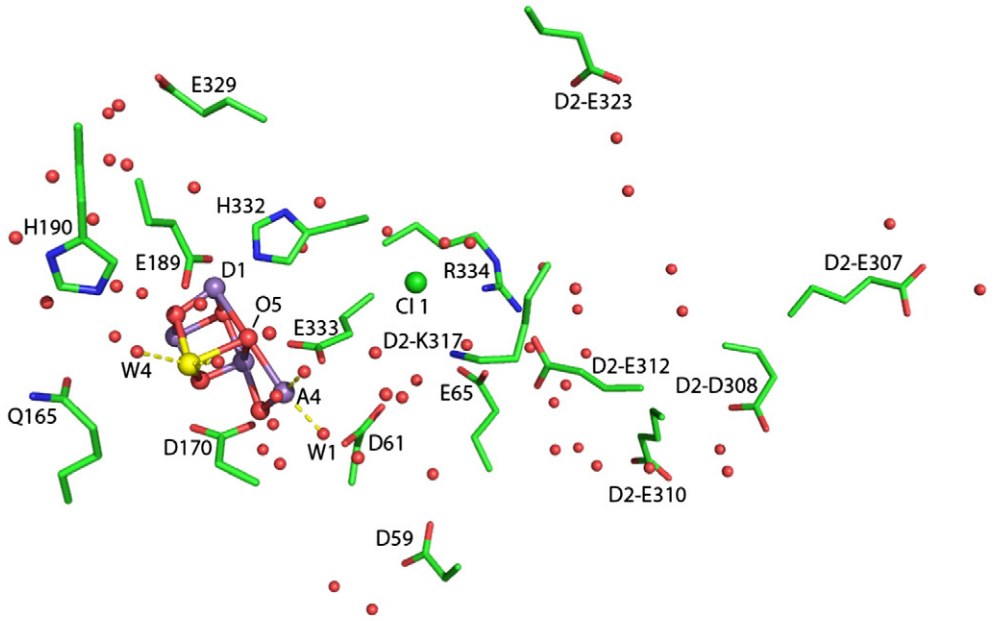

Fig. 6. The Mn_4CaO_5 cluster and selected nearby residues in the 1.9 Å structural model of PSII [12], including the cluster ligands D1-D170, D1-E189, D1-H332, and D1-E333. Except as noted otherwise, all residues are from the D1 polypeptide. Purple spheres, manganese ions; yellow sphere, calcium; green sphere, chloride; large red spheres, μ-oxo bridges; small red spheres, water molecules. The dangling Mn_{A4} ion, oxygen O5, and two of the cluster's water ligands (W1 and W4) are labeled.
Adapted with permission from Ref. [125]. Copyright 2004, American Chemical Society.

water molecules in the 1.9 Å structural model of PSII [12,53,54]. The mutation of any of these four residues [54,124–126,178–181], or the over-dehydration of wild-type samples [87], substantially decreases the efficiency of the S state transitions. On the basis of these observations, it was proposed that D1-D61, D1-E65, D2-E312, and D1-R334 form part of a dominant proton egress pathway leading from the Mn_4CaO_5 cluster to the lumen [124,125]. The mutation of residues in this putative proton egress pathway produces far more perturbations to the S_{n+1}-*minus*-S_n FTIR difference spectra than mutation of any of the carboxylate ligands of the Mn_4CaO_5 cluster. For example, the amplitudes of the carboxylate and amide II features at 1586(+), 1552(+), 1543(−) and 1509(+) cm^{-1} in the S_2-*minus*-S_1 FTIR difference spectrum are substantially diminished in D1-D61A, D1-E65A, D2-E312Q, and D1-R334A PSII core complexes and in overly-dehydrated samples [124,125] (for example, see Fig. 2). These spectral changes may reflect similar perturbations of the polypeptide backbone that are caused by disruption of a common network of hydrogen bonds. Similarly, a derivative feature at 1530(+)/1522(−) cm^{-1} in the S_2-*minus*-S_1 FTIR difference spectrum is eliminated by the D1-D61A, D2-E312A, and D1-R334A mutations [124–126] and by mutations of residues that coordinate the nearby $Cl^-(1)$ ion, such as D2-K317A [167] and D1-N181A (R.J.D., unpublished). The elimination of the same feature by mutations constructed at D1-D61, D1-N181, D1-R334, D2-E312, and D2-K317 suggests the partial disruption of a common network of hydrogen bonds that includes D1-D61 and the $Cl^-(1)$ ion.

3.3. Highly polarized hydrogen bonds — the region between 3100 and 2150 cm^{-1}

A broad feature centered at 3000 cm^{-1} in the S_2-*minus*-S_1 FTIR difference spectrum of PSII core complexes from *T. elongatus* has been assigned to changes in the polarization of a highly polarized network of strong hydrogen bonds (known as Zundel polarizability) near the Mn_4CaO_5 cluster [47,164]. Similar broad features in the S_3-*minus*-S_2, S_0-*minus*-S_3, and S_1-*minus*-S_0 spectra, centered at 2700, 2550, and 2600 cm^{-1}, respectively, were assigned to the same origin [47,164]. These features were sharply diminished or eliminated by hydration with $D_2^{16}O$ [164]. The higher frequency of the features in the S_2-*minus*-S_1 spectrum was attributed to the Mn_4CaO_5 cluster's lack of deprotonation during the S_1 to S_2 transition: compared to the other S state transitions, the extra proton would strengthen the hydrogen bond network, providing lower frequency features. Similar features have been observed in PSII core complexes from *Synechocystis* sp. PCC 6803 [126]. In the latter organism, hydration with $D_2^{16}O$ diminishes the broad feature in the S_2-*minus*-S_1 spectrum, but the broad features in the other S_{n+1}-*minus*-S_n difference spectra were obscured by O – D stretching modes after hydration with $D_2^{16}O$ or $D_2^{18}O$, preventing confirmation that these broad features are diminished by hydration with $D_2^{16}O$ or $D_2^{18}O$ [126].

The broad feature in the S_2-*minus*-S_1 FTIR difference spectrum was eliminated by the D1-D61A mutation [126] (Fig. 7). Its absence was confirmed by the similarity of the mutant spectrum (hydrated with $H_2^{16}O$) to the spectrum of the mutant after hydration with $D_2^{16}O$ or $D_2^{18}O$: evidently, no broad feature remained in the mutant to be eliminated by deuteration. It was concluded that the highly polarizable network of hydrogen bonds whose polarizability or protonation state increases during the S_1 to S_2 transition involves D1-D61. Because the broad feature centered near 2600 cm^{-1} in the wild-type S_3-*minus*-S_2 spectrum remained present in the mutant (albeit with a lower amplitude), it was concluded that the highly polarizable network of hydrogen bonds whose polarizability or protonation state increases during the S_2 to S_3 transition does not include D1-D61 [126].

It was reported recently that a substrate-containing cluster of five water molecules accepts a proton from the Mn_4CaO_5 cluster during the S_1 to S_2 transition [182]. This conclusion was based on the analysis of a broad positive feature at 2880 cm^{-1} in the S_2-*minus*-S_1 FTIR difference spectra of Ca-reconstituted spinach PSII core complexes. This feature undoubtedly corresponds to the broad feature in the S_2-*minus*-S_1 FTIR difference spectrum observed in PSII core complexes from *T. elongatus* [47,164] and *Synechocystis* sp. PCC 6803 [126]. In Ref. [182], this feature was eliminated by a variety of treatments including exchange of $H_2^{16}O$ for $D_2^{16}O$, extraction of Ca, replacement of Ca with Sr or Mg, and treatment with ammonia. However, the spectrum of Ca-reconstituted PSII presented in Ref. [182] lacks many of the features that are present in the corresponding S_2-*minus*-S_1 FTIR difference spectra of *T. elongatus* [47,83,164] and *Synechocystis* sp. PCC 6803 [126]. In *T. elongatus* and *Synechocystis* sp. PCC 6803, a wealth of features overlays

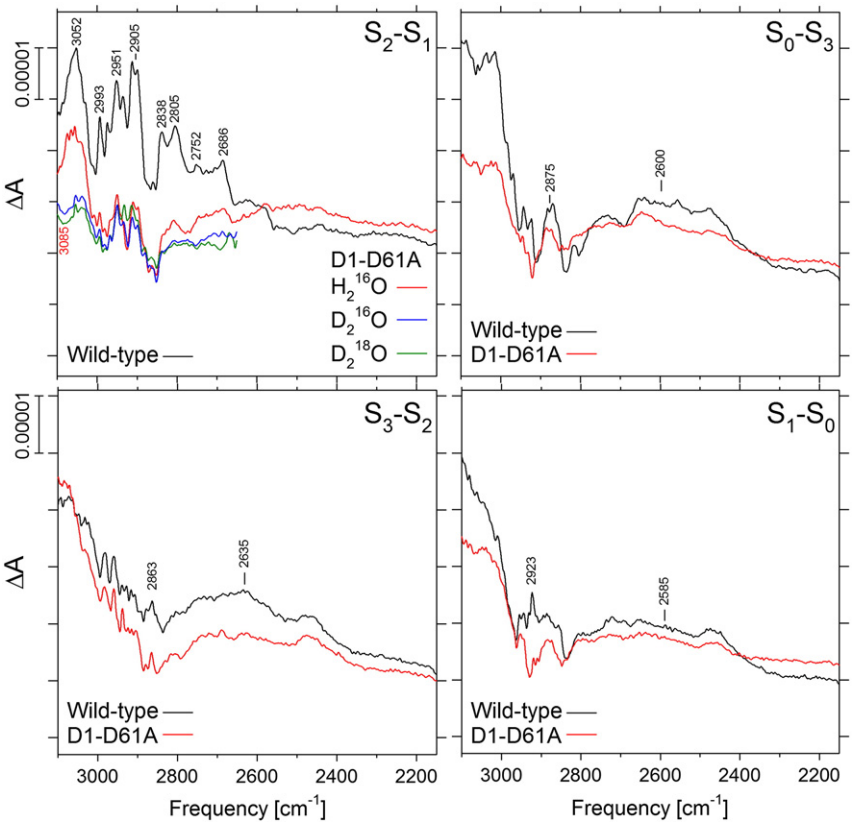

Fig. 7. Comparison of the FTIR difference spectra of wild-type (black) and D1-D61A (red) PSII core complexes between 3100 and 2150 cm^{-1} in response to four successive flash illuminations applied at 0 °C. The data in the upper left panel include the S_2-*minus*-S_1 FTIR difference spectra of D1-D61A between 3100 and 2650 cm^{-1} after hydration with $D_2^{16}O$ (blue) or $D_2^{18}O$ (green). The "S_0-*minus*-S_3" and "S_1-*minus*-S_0" spectra of D1-D61A probably correspond to a mixture of S state transitions .
Reprinted with permission from Ref. [126]. Copyright 2014, American Chemical Society.

the broad feature in the S_2-*minus*-S_1 spectrum (e.g., see Fig. 7, upper left panel). These features have been attributed to a mixture of C–H stretching vibrations from aliphatic groups and N–H stretching vibrations and their Fermi resonance overtones from the imidazole group(s) of one or more histidine residues [83,164,183]. Most of these features are missing from the S_2-*minus*-S_1 difference spectrum of Ca-reconstituted PSII presented in Ref. [182], especially after the exchange of $H_2^{16}O$ for $D_2^{18}O$. Unfortunately, the authors of Ref. [182] presented no mid-frequency FTIR difference spectra other than a schematic illustration of the S_2-*minus*-S_1 spectrum of presumably untreated spinach PSII core complexes. This omission makes it impossible for the reader to independently assess the quality of the treated samples after being dried onto the FTIR windows. In contrast to the data presented in Ref. [182], the broad feature was *not* eliminated by the replacement of Ca by Sr in *T. elongatus* (see Figure S5 of Ref. [39]) or *Synechocystis* sp. PCC 6803 (R.J. Debus, unpublished) and was not eliminated by treatment with ammonia in an earlier study of spinach PSII membranes (see Figure S5 of Ref. [39]). The omission of mid-frequency spectra in Ref. [182] also makes it impossible to independently assess the extent to which advancement to the S_3 or S_0 states was achieved in response to the appropriate number of actinic flashes. Although the authors of Ref. [182] attributed the negative features near 2880 cm^{-1} in their S_3-*minus*-S_2, S_0-*minus*-S_3, and S_1-*minus*-S_0 spectra to the deprotonation of a cationic water cluster during the S_2 to S_3, S_3 to S_0, and S_0 to S_1 transitions, they presented no $H_2^{16}O/D_2^{16}O$ exchange data to support the assignment of these features to vibrational modes of water molecules. In *T. elongatus* [164] and *Synechocystis* sp. PCC 6803 [126], the features near 2900 cm^{-1} in the S_3-*minus*-S_2, S_0-*minus*-S_3, and S_1-*minus*-S_0 spectra are largely insensitive to hydration with $D_2^{16}O$. Instead, $D_2^{16}O$-sensitive positive features centered at 2700, 2550, and 2600 cm^{-1} were reported [164]. These features were not observed in Ref. [182] as pointed out by the authors of Ref. [182] and demonstrated in their Figure S3. Regarding the absence of these features, it should be noted that the spectra of the weakly H-bonding O–H stretching region presented in Ref. [182] also contained no reproducible features above the baseline, as was also pointed out by the authors of Ref. [182] and also demonstrated in their Figure S3. In contrast, reproducible spectral features in this region have been presented by several laboratories in PSII core complexes isolated from *T. elongatus* [164,183,184], *Synechocystis* sp. PCC 6803 [102,108,126], and spinach [138] (see below, Section 4).

Broad features in the 3000–2000 cm^{-1} region that are sensitive to H_2O/D_2O exchange suggest the existence of one or more delocalized protons in a highly polarizable network of hydrogen bonds made up of amino acid side chains and water molecules [164,185–188]. The polarizability is caused by the fluctuations of protons within the network of hydrogen bonds. The extreme breath of the features is caused by strong interactions between the fluctuating protons and local electrostatic fields. The broad features that appear in all the S_{n+1}-*minus*-S_n spectra in Refs. [47,126,164] all have *positive* amplitudes. The positive amplitudes imply that the concentration and/or the polarizability of the protons in the network increases during each S state transition. It remains unclear whether the broad features originate from an increase of the polarizability of the protons in the network, from increased protonation of the network, or from a combination of both effects. Because the broad feature in the S_2-*minus*-S_1 spectrum is centered at a higher frequency than the features in the other transitions, a different combination of effects may take place during the S_1 to S_2 transition and may be related to the development of positive charge on the Mn_4CaO_5 cluster that is believed to accompany this transition on the basis of a variety of measurements [44,111–120]. The conclusion that a broad feature at 2880 cm^{-1} corresponds to a substrate-containing cluster of five water

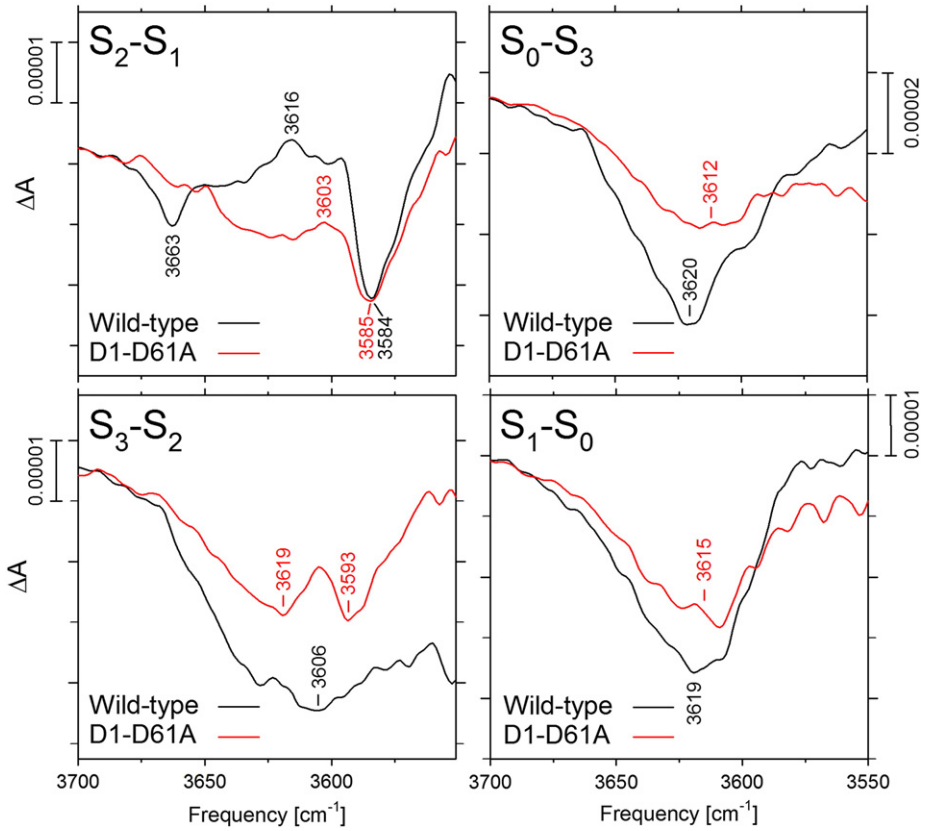

Fig. 8. Comparison of the FTIR difference spectra of wild-type (black) and D1-D61A (red) PSII core complexes in the weakly hydrogen bonded O – H stretching region in response to four successive flash illuminations applied at 0 °C. The "S_0-*minus*-S_3" and "S_1-*minus*-S_0" spectra of D1-D61A probably correspond to a mixture of S state transitions . Note the different vertical scales.
Reprinted with permission from Ref. [126]. Copyright 2014, American Chemical Society.

molecules that accepts a proton from the Mn_4CaO_5 cluster during the S_1 to S_2 transition and that deprotonates during the subsequent S state transitions [182] needs to be reassessed.

4. Weakly H-bonding OH stretching region

The high frequency region (3700–3500 cm^{-1}) includes the O – H stretching vibrations of water molecules participating in relatively weak hydrogen bonds. In PSII core complexes from *T. elongatus* [164,183,184] and spinach [138], the S_2-*minus*-S_1 FTIR difference spectrum exhibits a derivative-shaped feature having a negative peak at 3585–3588 cm^{-1} and a positive peak at 3613–3618 cm^{-1}. These peaks downshift ~12 cm^{-1} in the presence of $H_2^{18}O$ and 930–940 cm^{-1} in the presence of D_2O [183], confirming that they correspond to the O – H stretching vibrations of water molecules. On the basis of decoupling experiments employing a 1:1 mixture of H_2O and D_2O, the derivative-shaped feature was attributed to a water molecule coupled or bound to the Mn_4CaO_5 cluster that has an asymmetric hydrogen-bonding structure in the S_1 state and an even greater asymmetry of hydrogen-bonding in the S_2 state [183]. In the presence of ammonia, the two modes of this feature shift 2–3 cm^{-1}, showing that ammonia structurally perturbs this asymmetrically hydrogen-bonded water molecule, but does not replace it as a possible ligand to Mn [138]. In *T. elongatus*, the S_3-*minus*-S_2, S_0-*minus*-S_3, and S_1-*minus*-S_0 difference spectra exhibit broad negative features having minima at 3634, 3621, and 3612 cm^{-1}, respectively [164,184]. These features also downshift in the presence of $H_2^{18}O$ and D_2O and have been attributed to water molecules that are located on or near the Mn_4CaO_5 cluster and that either deprotonate or form stronger hydrogen bonds (i.e., weakly hydrogen-bonded OH groups become strongly hydrogen-bonded) during the S_2 to S_3, S_3 to S_0, and S_0 to S_1 transitions [164,184].

In the S_2-*minus*-S_1 difference spectrum of PSII core complexes from *Synechocystis* sp. PCC 6803, the negative and positive peaks discussed in the previous paragraph appear at 3584 cm^{-1} and 3616 cm^{-1} respectively, with the positive peak being less distinct than that in *T. elongatus* or spinach [102,108,126]. These peaks were substantially altered by the CP43–E354Q mutation [102], leading the authors of this study to conclude that the water molecule corresponding to these peaks binds to one of the Mn ions that is ligated by this residue. Interestingly, the exchange rates of the rapidly exchanging and slowly exchanging substrate water molecules in the S_3 state increased eight-fold and two-fold in this mutant [103].

The S_2-*minus*-S_1 difference spectrum in *Synechocystis* sp. PCC 6803 also contains a negative feature at 3663 cm^{-1} [108,126]. Only a weak vestige of this peak is present in *T. elongatus* [164,183] and it has not been reported in spinach [138]. This feature also downshifts in the presence of $H_2^{18}O$ and D_2O [108,126], confirming that it also corresponds to an O – H stretching vibration of a water molecule. This feature has been assigned to a water molecule on or near the Mn_4CaO_5 cluster that either deprotonates or forms a stronger hydrogen bond during the S_1 to S_2 transition [108,126]. The greater prominence of this feature in *Synechocystis* sp. PCC 6803 might be caused by a higher hydration of samples (99% Relative Humidity) compared to those examined in *T. elongatus* or spinach. The extent of sample hydration is known to substantially affect the amplitudes of features in the S_{n+1}-*minus*-S_n FTIR difference spectra [87,124,189]. The S_3-*minus*-S_2, S_0-minus-S_3, and S_1-*minus*-S_0 spectra in *Synechocystis* sp. PCC 6803 also exhibit broad negative features, although their minima are shifted slightly from those

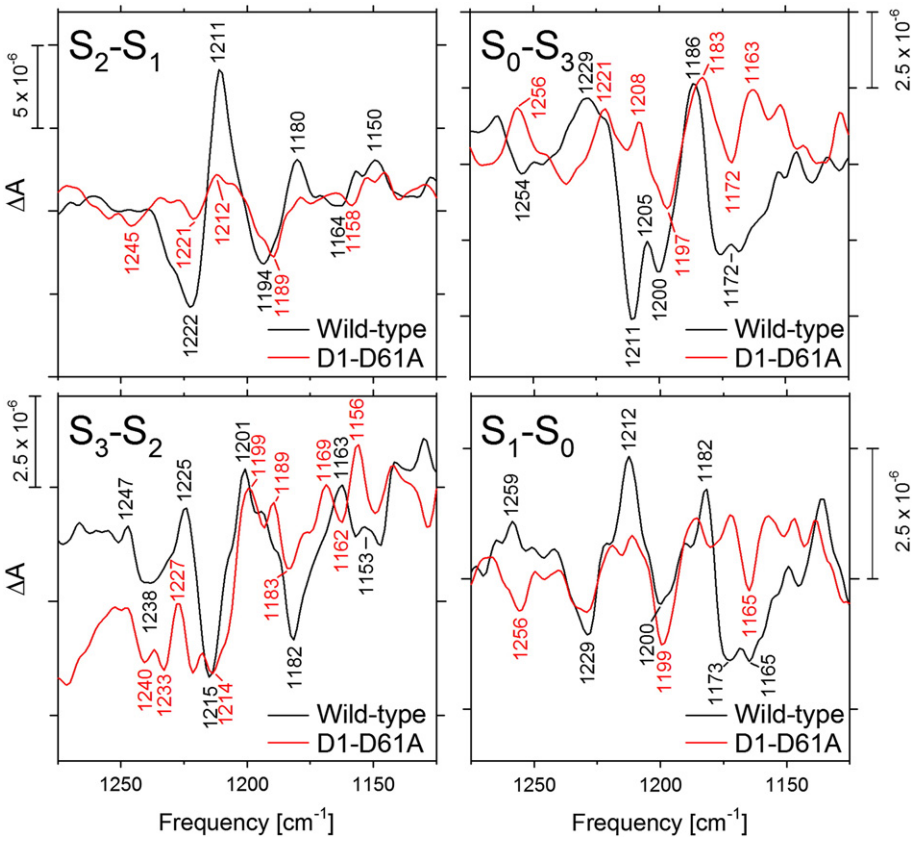

Fig. 9. Comparison of the $D_2^{16}O$-*minus*-$D_2^{18}O$ double difference spectra of wild-type (black) and D1-D61A (red) PSII core complexes between 1275 and 1125 cm^{-1} in response to four successive flashes applied at 0 °C. The "S_0-*minus*-S_3" and "S_1-*minus*-S_0" spectra of D1-D61A probably correspond to a mixture of S state transitions. Note the different vertical scales. Reprinted with permission from Ref. [126]. Copyright 2014, American Chemical Society.

observed in *T. elongatus*, particularly the minimum in the S_3-*minus*-S_2 spectrum [108,126]. These shifts may reflect slight differences between the networks of hydrogen bonds around the Mn_4CaO_5 cluster in the two species of cyanobacteria.

The D1-D61A mutation of *Synechocystis* sp. PCC 6803 eliminates the negative feature at 3663 cm^{-1} from the S_2-*minus*-S_1 spectrum and splits the broad negative feature in the S_3-*minus*-S_2 spectrum into separate minima at 3619 cm^{-1} and 3593 cm^{-1} (see Fig. 8). Because the negative feature at 3663 cm^{-1} corresponds to a water molecule on or near the Mn_4CaO_5 cluster that either deprotonates or forms a stronger hydrogen bond during the S_1 to S_2 transition, it was concluded that the hydrogen-bonding properties of this water molecule are altered by the mutation. This negative feature is also eliminated by the D1-E333Q [108] and D2-K317A (R.J.D., unpublished) mutations, but not by the D1-D170H mutation (R.J.D., unpublished), suggesting that the group in question may be a water molecule located near the $Cl^-(1)$ ion. The split of the broad negative feature in the S_3-*minus*-S_2 spectrum into two separate minima suggests that at least some of the water molecules that deprotonate or form stronger hydrogen bonds during the S_2 to S_3 transition are located near D1-D61.

5. DOD bending region

The H – O – H bending mode appears near 1640 cm^{-1}, is sensitive to hydrogen bonding, and disappears when the H_2O molecule is deprotonated [190]. Consequently, H – O – H bending modes would seem an attractive probe of water reactions in PSII. Unfortunately, these modes are weak and the 1640 cm^{-1} region overlaps the strong absorption bands of the amide I groups of the polypeptide backbone. However, the D – O – D bending mode can be monitored near 1210 cm^{-1}, a region that is practically devoid of other protein vibrational modes [190]. The D – O – D bending modes are also weak. Consequently, they are best observed in $D_2^{16}O$-*minus*-$D_2^{18}O$ double difference spectra [190]. Such spectra have been reported in PSII core complexes from *T. elongatus* [190] and *Synechocystis* sp. PCC 6803 [126] for all the S state transitions (Fig. 9). In a $D_2^{16}O$-*minus*-$D_2^{18}O$ double difference spectrum, the alteration of a single D – O – D bending mode during an S state transition will cause four peaks to appear (two from $D_2^{16}O$ and two from $D_2^{18}O$). In contrast, if a D_2O molecule deprotonates during a transition, the bending mode will disappear and only two peaks will appear in the double difference spectrum. One complication is that some positive and negative peaks may overlap and cancel their intensities, decreasing the number of bands observed. In *T. elongatus*, six to eight peaks were observed for each S state transition [190] and at least four peaks were observed in similar spectra obtained in *Synechocystis* sp. PCC 6803 (Fig. 9) [126]. The observations imply that up to two D_2O molecules have their D – O – D bending modes altered during each S state transition. These D_2O molecules likely reside in the first or second coordination sphere of the Mn_4CaO_5 cluster or in a nearby network of hydrogen bonds. Most of the peaks in the double difference spectra oscillate during the S state transitions, implying that most of the alterations to the D – O – D bending modes are reversed during the S state cycle. However, negative features near 1240 cm^{-1} in the S_3-*minus*-S_2 and S_0-*minus*-S_3 double difference spectra have no apparent positive counterparts in the other double difference spectra.

These were attributed to substrate water molecules that insert into the Mn_4CaO_5 cluster from a cluster of water molecules within PSII during the S_2 to S_3 and S_3 to S_0 transitions [190], although these water molecules may bind to "holding" sites and become substrate on the next turnover.

The D1-D61A mutation eliminates the 1222(−), 1211(+), and 1180(+) features from the $D_2^{16}O$-*minus*-$D_2^{18}O$ double difference spectrum of the S_1 to S_2 transition in *Synechocystis* sp. PCC 6803 (Fig. 9, upper left panel) [126]. It was concluded that one of the D_2O molecules whose D–O–D bending mode changes during the S_1 to S_2 transition is no longer present in the mutant and that this D_2O molecule forms a hydrogen bond to D1-D61 in wild-type PSII [126]. The absence of this H_2O molecule in D1-D61A may impede proton egress from the Mn_4CaO_5 cluster, thereby contributing to the decreased efficiency of the S state transitions in this mutant. Most of the features that are present in the $D_2^{16}O$-*minus*-$D_2^{18}O$ double difference spectrum of the S_2 to S_3 transition in wild-type PSII appear to be present in the spectrum of the mutant (Fig. 9, lower left panel). Consequently, it seems likely that the D_2O molecules whose D–O–D bending modes change during the S_2 to S_3 transition do not interact directly with D1-D61.

6. Concluding remarks

Light-induced FTIR difference spectroscopy has become one of the primary tools for investigating the mechanism of photosynthetic water oxidation because of its utility in detecting changes in bond strengths and hydrogen bond structures. Studies published over the last two decades have provided information about structural changes that occur during the O_2-evolving catalytic cycle, including those involving the Mn_4CaO_5 cluster's core and amino acid ligands, nearby networks of hydrogen bonds, and nearby water molecules. The crystallographic structural models of PSII, especially the recent 1.9 Å structural model [12,13] and its computational refinements [14–19], have dramatically improved the power of FTIR spectroscopy to provide mechanistic insight by serving as invaluable guides for studies designed to elucidate the roles of specific amino acid residues participating in networks of hydrogen bonds comprising substrate (water) access and proton egress pathways and interacting with specific water molecules, including substrate. Assigning spectral features to specific water molecules and characterizing the interactions of these water molecules with nearby residues is crucial for understanding mechanism and attempts to make these assignments are just beginning. Both static FTIR difference spectroscopy (reviewed here) and time resolved IR studies (e.g., [47], reviewed elsewhere in this issue [77]), will play increasingly crucial roles in elucidating mechanistic details, complementing computational studies (e.g., [14–22,24–30,32,140,163]) and information obtained by X-ray crystallography (e.g., [191,192]), spectroscopic methods such as EPR (e.g. [23,26,27]) and X-ray absorption (e.g., [31,192]), and other methods such as time-resolved membrane inlet mass spectrometry (TR-MIMS) (e.g., [9,193,194]).

Acknowledgements

The author thanks Takumi Noguchi for helpful discussions and for sending preprints of unpublished work. Work in the author's laboratory is supported by the Department of Energy, Office of Basic Energy Sciences, Division of Chemical Sciences (grant DE-FG02-10ER16191).

References

[1] T. Cardona, A. Sedoud, N. Cox, A.W. Rutherford, Charge separation in Photosystem II: a comparative and evolutionary overview, Biochim. Biophys. Acta 1817 (2012) 26–43.
[2] J. Barber, Photosystem II: the water-splitting enzyme of photosynthesis, Cold Spring Harb. Symp. Quant. Biol. 77 (2012) 295–307.
[3] L.-X. Shi, M. Hall, C. Funk, W.P. Schröder, Photosystem II, a growing complex: updates on newly discovered components and low molecular mass proteins, Biochim. Biophys. Acta 1817 (2012) 13–25.
[4] D.J. Vinyard, G.M. Ananyev, G.C. Dismukes, Photosystem II: the reaction center of oxygenic photosynthesis, Annu. Rev. Biochem. 82 (2013) 577–606.
[5] J. Messinger, T. Noguchi, J. Yano, Photosynthetic O_2 evolution, in: T. Wydrzynski, W. Hillier (Eds.), Molecular Solar Fuels, Royal Society of Chemistry, Cambridge, UK, 2012, pp. 163–207.
[6] G. Renger, Mechanism of light induced water splitting in Photosystem II of oxygen evolving photosynthetic organisms, Biochim. Biophys. Acta 1817 (2012) 1164–1176.
[7] H. Dau, I. Zaharieva, M. Haumann, Recent developments in research on water oxidation by Photosystem II, Curr. Opin. Chem. Biol. 16 (2012) 3–10.
[8] N. Cox, D.A. Pantazis, F. Neese, W. Lubitz, Biological water oxidation, Acc. Chem. Res. 46 (2013) 1588–1596.
[9] N. Cox, J. Messinger, Reflections on substrate water and dioxygen formation, Biochim. Biophys. Acta 1827 (2013) 1020–1030.
[10] R. Pokhrel, G.W. Brudvig, Oxygen-evolving complex of Photosystem II: correlating structure with spectroscopy, Phys. Chem. Chem. Phys. 16 (2014) 11812–11821.
[11] J. Yano, V.K. Yachandra, Mn_4Ca cluster in photosynthesis: where and how water is oxidized to dioxygen, Chem. Rev. 114 (2014) 4175–4250.
[12] Y. Umena, K. Kawakami, J.-R. Shen, N. Kamiya, Crystal structure of oxygen-evolving Photosystem II at a resolution of 1.9 Å, Nature 473 (2011) 55–60.
[13] K. Kawakami, Y. Umena, N. Kamiya, J.-R. Shen, Structure of the catalytic, inorganic core of oxygen-evolving Photosystem II at 1.9 Å resolution, J. Photochem. Photobiol. B Biol. 104 (2011) 9–18.
[14] S. Luber, I. Rivalta, Y. Umena, K. Kawakami, J.-R. Shen, N. Kamiya, G.W. Brudvig, V.S. Batista, S_1-state model of the O_2-evolving complex of Photosystem II, Biochemistry 50 (2011) 6308–6311.
[15] W. Ames, D.A. Pantazis, V. Krewald, N. Cox, J. Messinger, W. Lubitz, F. Neese, Theoretical evaluation of structural models of the S_2 state in the oxygen evolving complex of Photosystem II: protonation states and magnetic interactions, J. Am. Chem. Soc. 133 (2011) 19743–19757.
[16] P.E.M. Siegbahn, The effect of backbone constraints: the case of water oxidation by the oxygen-evolving complex in PSII, ChemPhysChem 12 (2011) 3274–3280.
[17] M. Kusunoki, S_1-state Mn_4Ca complex of Photosystem II exists in equilibrium between the two most-stable isomeric substates: XRD and EXAFS evidence, J. Photochem. Photobiol. B Biol. 104 (2011) 100–110.
[18] A. Galstyan, A. Robertazzi, E.W. Knapp, Oxygen-evolving Mn cluster in Photosystem II: the protonation pattern and oxidation state in the high-resolution crystal structure, J. Am. Chem. Soc. 134 (2012) 7442–7449.
[19] H. Isobe, M. Shoji, S. Yamanaka, Y. Umena, K. Kawakami, N. Kamiya, J.-R. Shen, K. Yamaguchi, Theoretical illumination of water-inserted structures of the $CaMn_4O_5$ cluster in the S_2 and S_3 states of oxygen-evolving complex of Photosystem II: full geometry optimizations by B3LYP hybrid density functional, Dalton Trans. 41 (2012) 13727–13740.
[20] P.E.M. Siegbahn, Structures and energetics for O_2 formation in Photosystem II, Acc. Chem. Res. 42 (2009) 1871–1880.
[21] S. Yamanaka, H. Isobe, K. Kanda, T. Saito, Y. Umena, K. Kawakami, J.-R. Shen, N. Kamiya, M. Okamura, H. Nakamura, K. Yamaguchi, Possible mechanisms for the O–O bond formation in oxygen evolution reaction at the $CaMn_4O_5(-H_2O)_4$ cluster of PSII refined to 1.9 Å resolution, Chem. Phys. Lett. 511 (2011) 138–145.
[22] P.E.M. Siegbahn, Mechanisms for proton release during water oxidation in the S_2 to S_3 and S_3 to S_4 transitions in Photosystem II, Phys. Chem. Chem. Phys. 14 (2012) 4849–4856.
[23] L. Rapatskiy, N. Cox, A. Savitsky, W.M. Ames, J. Sander, M.M. Nowaczyk, M. Rögner, A. Boussac, F. Neese, J. Messinger, W. Lubitz, Detection of water-binding sites of the oxygen-evolving complex of Photosystem II using W-band ^{17}O electron-electron double resonance-detected NMR spectroscopy, J. Am. Chem. Soc. 134 (2012) 16619–16634.
[24] P.E.M. Siegbahn, Water oxidation mechanism in Photosystem II, including oxidations, proton release pathways, O–O bond formation and O_2 release, Biochim. Biophys. Acta 1827 (2013) 1003–1019.
[25] P.E.M. Siegbahn, Substrate water exchange of the oxygen evolving complex in PSII in the S_1, S_2, and S_3 states, J. Am. Chem. Soc. 135 (2013) 9442–9449.
[26] M. Pérez Navarro, W.M. Ames, H. Nilsson, T. Lohmiller, D.A. Pantazis, L. Rapatskiy, M.M. Nowaczyk, F. Neese, A. Boussac, J. Messinger, W. Lubitz, N. Cox, Ammonia binding to the oxygen-evolving complex of Photosystem II identified the solvent-exchangeable oxygen bridge (μ-oxo) of the manganese tetramer, Proc. Natl. Acad. Sci. U. S. A. 110 (2013) 15561–15566.
[27] T. Lohmiller, V. Krewald, M. Pérez Navarro, M. Retegan, L. Rapatskiy, M.M. Nowaczyk, A. Boussac, F. Neese, W. Lubitz, D.A. Pantazis, N. Cox, Structure, ligands and substrate coordination of the oxygen-evolving complex of Photosystem II in the S_2 state: a combined EPR and DFT study, Phys. Chem. Chem. Phys. 16 (2014) 11877–11892.
[28] D.A. Pantazis, W. Ames, N. Cox, W. Lubitz, F. Neese, Two interconvertable structures that explain the spectroscopic properties of the oxygen-evolving complex of Photosystem II in the S_2 state, Angew. Chem. Int. Ed. 51 (2012) 9935–9940.
[29] K. Saito, H. Ishikita, Influence of the Ca^{2+} ion on the Mn_4Ca conformation and the H-bond network arrangement in Photosystem II, Biochim. Biophys. Acta 1837 (2014) 159–166.
[30] D. Bovi, D. Narzi, L. Guidoni, The S_2 state of the oxygen-evolving complex of Photosystem II explored by QM/MM dynamics: spin surfaces and metastable states suggest a reaction path towards the S_3 state, Angew. Chem. Int. Ed. 52 (2013) 11744–11749.

[31] C. Glöckner, J. Kern, M. Broser, A. Zouni, V.K. Yachandra, J. Yano, Structural changes of the oxygen-evolving complex in Photosystem II during the catalytic cycle, J. Biol. Chem. 288 (2013) 22607–22620.
[32] D. Narzi, D. Bovi, L. Guidoni, Pathway for Mn-cluster oxidation by tyrosine-Z in the S_2 state of Photosystem II, Proc. Natl. Acad. Sci. U. S. A. 111 (2014) 8723–8728.
[33] J.P. McEvoy, G.W. Brudvig, Water-splitting chemistry of Photosystem II, Chem. Rev. 106 (2006) 4455–4483.
[34] H. Dau, M. Haumann, Eight steps preceding O – O bond formation in oxygenic photosynthesis — a basis reaction cycle of the Photosystem II manganese complex, Biochim. Biophys. Acta 1767 (2007) 472–483.
[35] H. Dau, M. Haumann, The manganese complex of Photosystem II in its reaction cycle — basic framework and possible realization at the atomic level, Coord. Chem. Rev. 252 (2008) 273–295.
[36] E.M. Sproviero, J.A. Gascón, J.P. McEvoy, G.W. Brudvig, V.S. Batista, Quantum mechanics/molecular mechanics study of the catalytic cycle of water splitting in Photosystem II, J. Am. Chem. Soc. 130 (2008) 3428–3442.
[37] H. Dau, C. Limberg, T. Reier, M. Risch, S. Roggan, P. Strasser, The mechanism of water oxidation: from electrolysis via homogeneous to biological catalysis, ChemCatChem 2 (2010) 724–761.
[38] A. Klauss, M. Haumann, H. Dau, Alternating electron and proton transfer steps in photosynthetic water oxidation, Proc. Natl. Acad. Sci. U. S. A. 109 (2012) 16035–16040.
[39] S. Nakamura, R. Nagao, R. Takahashi, T. Noguchi, Fourier transform infrared detection of a polarizable proton trapped between photooxidized tyrosine Y_Z and a coupled histidine in Photosystem II: relevance to the proton transfer mechanism of water oxidation, Biochemistry 53 (2014) 3131–3144.
[40] J.P. McEvoy, G.W. Brudvig, Structure-based mechanism of photosynthetic water oxidation, Phys. Chem. Chem. Phys. 6 (2004) 4754–4763.
[41] H. Ishikita, E.-W. Knapp, Function of redox-active tyrosine in Photosystem II, Biophys. J. 90 (2006) 3886–3896.
[42] M. Haumann, P. Liebisch, C. Müller, M. Barra, M. Grabolle, H. Dau, Photosynthetic O_2 formation tracked by time-resolved X-ray experiments, Science 310 (2005) 1019–1021.
[43] H. Dau, M. Haumann, Time resolved X-ray spectroscopy leads to an extension of the classical S-state cycle model of photosynthetic oxygen evolution, Photosynth. Res. 92 (2007) 327–343.
[44] F. Rappaport, M. Blanchard-Desce, J. Lavergne, Kinetics of electron transfer and electrochromic change during the redox transitions of the photosynthetic oxygen-evolving complex, Biochim. Biophys. Acta 1184 (1994) 178–192.
[45] L. Gerencsér, H. Dau, Water oxidation by Photosystem II: H_2O–D_2O exchange and the influence of pH support formation of an intermediate by removal of a proton before dioxygen creation, Biochemistry 49 (2010) 10098–10106.
[46] F. Rappaport, N. Ishida, M. Sugiura, A. Boussac, Ca^{2+} determines the entropy changes associated with the formation of transition states during water oxidation by Photosystem II, Energy Environ. Sci. 4 (2011) 2520–2524.
[47] T. Noguchi, H. Suzuki, M. Tsuno, M. Sugiura, C. Kato, Time-resolved infrared detection of the proton and protein dynamics during photosynthetic oxygen evolution, Biochemistry 51 (2012) 3205–3214.
[48] K.N. Ferreira, T.M. Iverson, K. Maghlaoui, J. Barber, S. Iwata, Architecture of the photosynthetic oxygen-evolving center, Science 303 (2004) 1831–1838.
[49] B. Loll, J. Kern, W. Saenger, A. Zouni, J. Biesiadka, Towards complete cofactor arrangement in the 3.0 Å resolution structure of Photosystem II, Nature 438 (2005) 1040–1044.
[50] A. Guskov, J. Kern, A. Gabdulkhakov, M. Broser, A. Zouni, W. Saenger, Cyanobacterial Photosystem II at 2.9-Å resolution and the role of quinones, lipids, channels, and chloride, Nat. Struct. Mol. Biol. 16 (2009) 334–342.
[51] J. Barber, K.N. Ferreira, K. Maghlaoui, S. Iwata, Structural model of the oxygen-evolving centre of Photosystem II with mechanistic implications, Phys. Chem. Chem. Phys. 6 (2004) 4737–4742.
[52] J. De Las Rivas, J. Barber, Analysis of the structure of the PsbO protein and its implications, Photosynth. Res. 81 (2004) 329–343.
[53] A.-N. Bondar, H. Dau, Extended protein/water H-bond networks in photosynthetic water oxidation, Biochim. Biophys. Acta 1817 (2012) 1177–1190.
[54] K. Linke, F.M. Ho, Water in Photosystem II: structural, functional, and mechanistic considerations, Biochim. Biophys. Acta 1837 (2014) 14–32.
[55] H. Ishikita, W. Saenger, B. Loll, J. Biesiadka, E.-W. Knapp, Energetics of a possible proton exit pathway for water oxidation in Photosystem II, Biochemistry 45 (2006) 2063–2071.
[56] F.M. Ho, S. Styring, Access channels and methanol binding site to the $CaMn_4$ cluster in Photosystem II based on solvent accessibility simulation, with implications for substrate water access, Biochim. Biophys. Acta 1777 (2008) 140–153.
[57] J.W. Murray, J. Barber, Structural characteristics of channels and pathways in Photosystem II including the identification of an oxygen channel, J. Struct. Biol. 159 (2007) 228–237.
[58] A. Gabdulkhakov, A. Guskov, M. Broser, J. Kern, F. Müh, W. Saenger, A. Zouni, Probing the accessibility of the Mn_4Ca cluster in Photosystem II: channels calculation, noble gas derivatization, and cocrystallization with DMSO, Structure 17 (2009) 1223–1234.
[59] S. Vassiliev, P. Comte, A. Mahboob, D. Bruce, Tracking the flow of water through Photosystem II using molecular dynamics and streamline tracing, Biochemistry 49 (2010) 1873–1881.
[60] S. Vassiliev, T. Zaraiskaya, D. Bruce, Exploring the energetics of water permeation in Photosystem II by multiple steered molecular dynamics simulations, Biochim. Biophys. Acta 1817 (2012) 1671–1678.
[61] S. Vassiliev, T. Zaraiskaya, D. Bruce, Molecular dynamics simulations reveal highly permeable oxygen exit channels shared with water uptake channels in Photosystem II, Biochim. Biophys. Acta 1827 (2013) 1148–1155.
[62] K. Ogata, T. Yuki, M. Hatakeyama, W. Uchida, S. Nakamura, All-atom molecular dynamics simulation of Photosystem II embedded in thylakoid membranes, J. Am. Chem. Soc. 135 (2013) 15670–15673.
[63] L.K. Frankel, L. Sallans, P.A. Limbach, T.M. Bricker, Identification of oxidized amino acid residues in the vicinity of the Mn_4CaO_5 cluster of Photosystem II: implications for the identification of oxygen channels within the photosystem, Biochemistry 51 (2012) 6371–6377.
[64] L.K. Frankel, L. Sallans, H. Bellamy, J.S. Goettert, P.A. Limbach, T.M. Bricker, Radiolytic mapping of solvent-contact surfaces in Photosystem II of higher plants, J. Biol. Chem. 288 (2013) 23565–23572.
[65] F.M. Ho, Uncovering channels in Photosystem II by computer modeling: current progress, future prospects, and lessons from analogous systems, Photosynth. Res. 98 (2008) 503–522.
[66] F.M. Ho, Substrate and proton channels in Photosystem II, in: T. Wydrzynski, W. Hillier (Eds.), Molecular Solar Fuels, Royal Society of Chemistry, Cambridge, UK, 2012, pp. 208–248.
[67] F.M. Ho, Structural and mechanistic investigations of Photosystem II through computational methods, Biochim. Biophys. Acta 1817 (2012) 106–120.
[68] C. Zscherp, A. Barth, Reaction-induced infrared difference spectroscopy for the study of protein reaction mechanisms, Biochemistry 40 (2001) 1875–1883.
[69] A. Barth, C. Zscherp, What vibrations tell us about proteins, Q. Rev. Biophys. 35 (2002) 369–430.
[70] P.R. Rich, M. Iwaki, Infrared protein spectroscopy as a tool to study protonation reactions within proteins, in: M. Wikström (Ed.), Biophysical and Structural Aspects of Bioenergetics, Royal Society of Chemistry, Cambridge, U.K., 2005, pp. 314–333.
[71] A. Barth, Infrared spectroscopy of proteins, Biochim. Biophys. Acta 1767 (2007) 1073–1101.
[72] C. Berthomieu, R. Hienerwadel, Fourier Transform Infrared (FTIR) spectroscopy, Photosynth. Res. 101 (2009) 157–170.
[73] T. Noguchi, Light-induced FTIR difference spectroscopy as a powerful tool toward understanding the molecular mechanism of photosynthetic oxygen evolution, Photosynth. Res. 91 (2007) 59–69.
[74] T. Noguchi, Fourier transform infrared analysis of the photosynthetic oxygen-evolving center, Coord. Chem. Rev. 251 (2008) 336–346.
[75] H.-A. Chu, Fourier transform infrared difference spectroscopy for studying the molecular mechanism of photosynthetic water oxidation, Frontiers Plant Sci. 4 (2013) 146.
[76] T. Noguchi, Monitoring the reactions of photosynthetic water oxidation using infrared spectroscopy, Biomed. Spectrosc. Imaging 2 (2013) 115–128.
[77] T. Noguchi, Fourier transform infrared difference and time-resolved infrared detection of the electron and proton transfer dynamics in photosynthetic water oxidation, Biochim. Biophys. Acta 1847 (2015) 35–45.
[78] T. Noguchi, T.-A. Ono, Y. Inoue, Detection of structural changes upon S_1-to-S_2 transition in the oxygen-evolving manganese cluster in Photosystem II by light-induced Fourier transform infrared difference spectroscopy, Biochemistry 31 (1992) 5953–5956.
[79] T. Noguchi, T.-A. Ono, Y. Inoue, Direct detection of a carboxylate bridge between Mn and Ca^{2+} in the photosynthetic oxygen-evolving center by means of Fourier transform infrared spectroscopy, Biochim. Biophys. Acta 1228 (1995) 189–200.
[80] T. Noguchi, T.-A. Ono, Y. Inoue, A carboxylate ligand interacting with water in the oxygen-evolving center of Photosystem II as revealed by Fourier transform infrared spectroscopy, Biochim. Biophys. Acta 1232 (1995) 59–66.
[81] T. Noguchi, Y. Inoue, X.S. Tang, Structural coupling between the oxygen-evolving Mn cluster and a tyrosine residue in Photosystem II as revealed by Fourier transform infrared spectroscopy, Biochemistry 36 (1997) 14705–14711.
[82] H.-A. Chu, M.T. Gardner, J.P. O'Brien, G.T. Babcock, Low-frequency Fourier transform infrared spectroscopy of the oxygen-evolving and quinone acceptor complexes in Photosystem II, Biochemistry 38 (1999) 4533–4541.
[83] T. Noguchi, Y. Inoue, X.-S. Tang, Structure of a histidine ligand in the photosynthetic oxygen-evolving complex as studied by light-induced Fourier transform infrared spectroscopy, Biochemistry 38 (1999) 10187–10195.
[84] H.-A. Chu, W. Hillier, N.A. Law, H. Sackett, S. Haymond, G.T. Babcock, Light-induced FTIR difference spectroscopy of the S_2 to S_3 transition of the oxygen-evolving complex in Photosystem II, Biochim. Biophys. Acta 1459 (2000) 528–532.
[85] T. Noguchi, M. Sugiura, Flash-induced Fourier transform infrared detection of the structural changes during the S-state cycle of the oxygen-evolving complex in Photosystem II, Biochemistry 40 (2001) 1497–1502.
[86] W. Hillier, G.T. Babcock, S-state dependent FTIR difference spectra for the Photosystem II oxygen evolving complex, Biochemistry 40 (2001) 1503–1509.
[87] T. Noguchi, M. Sugiura, Flash-induced FTIR difference spectra of the water oxidizing complex in moderately hydrated Photosystem II core films: effect of hydration extent on S-state transitions, Biochemistry 41 (2002) 2322–2330.
[88] T. Noguchi, M. Sugiura, Y. Inoue, FTIR studies on the amino-acid ligands of the photosynthetic oxygen-evolving Mn-cluster, in: K. Itoh, M. Tasumi (Eds.), Fourier Transform Spectroscopy: Twelfth International Conference, Waseda University Press, Tokyo, Japan, 1999, pp. 459–460.
[89] T. Noguchi, M. Sugiura, Analysis of flash-induced FTIR difference spectra of the S-state cycle in the photosynthetic water-oxidizing complex by uniform ^{15}N and ^{13}C isotope labeling, Biochemistry 42 (2003) 6035–6042.
[90] Y. Kimura, N. Mizusawa, A. Ishii, T. Yamanari, T.-A. Ono, Changes of low-frequency vibrational modes induced by universal ^{15}N- and ^{13}C-isotope labeling in S_2/S_1 FTIR

difference spectrum of oxygen-evolving complex, Biochemistry 42 (2003) 13170–13177.
[91] T. Yamanari, Y. Kimura, N. Mizusawa, A. Ishii, T.-A. Ono, Mid- to low-frequency Fourier transform infrared spectra of S-state cycle for photosynthetic water oxidation in *Synechocystis* sp. PCC 6803, Biochemistry 43 (2004) 7479–7490.
[92] Y. Kimura, N. Mizusawa, A. Ishii, T.-A. Ono, FTIR detection of structural changes in a histidine ligand during S-state cycling of photosynthetic oxygen-evolving complex, Biochemistry 44 (2005) 16072–16078.
[93] P.J. Nixon, J.T. Trost, B.A. Diner, Role of the carboxy terminus of polypeptide D1 in the assembly of a functional water-oxidizing manganese cluster in Photosystem II of the cyanobacterium *Synechocystis* sp. PCC 6803: assembly requires a free carboxyl group at C-terminal position 344, Biochemistry 31 (1992) 10859–10871.
[94] H.-A. Chu, W. Hillier, R.J. Debus, Evidence that the C-terminus of the D1 polypeptide is ligated to the manganese ion that undergoes oxidation during the S_1 to S_2 transition: an isotope-edited FTIR study, Biochemistry 43 (2004) 3152–3166.
[95] Y. Kimura, N. Mizusawa, T. Yamanari, A. Ishii, T.-A. Ono, Structural changes of D1 C-terminal α-carboxylate during S-state cycling of photosynthetic oxygen evolution, J. Biol. Chem. 280 (2005) 2078–2083.
[96] R.J. Debus, Protein ligation of the photosynthetic oxygen-evolving center, Coord. Chem. Rev. 252 (2008) 244–258.
[97] M.A. Strickler, L.M. Walker, W. Hillier, R.J. Debus, Evidence from biosynthetically incorporated strontium and FTIR difference spectroscopy that the C-terminus of the D1 polypeptide of Photosystem II does not ligate calcium, Biochemistry 44 (2005) 8571–8577.
[98] E.M. Sproviero, J.A. Gascón, J.P. McEvoy, G.W. Brudvig, V.S. Batista, QM/MM models of the O_2-evolving complex of Photosystem II, J. Chem. Theory Comput. 2 (2006) 1119–1134.
[99] E.M. Sproviero, J.A. Gascón, J.P. McEvoy, G.W. Brudvig, V.S. Batista, Computation studies of the O_2-evolving complex of Photosystem II and biomimetic oxomanganese complexes, Coord. Chem. Rev. 252 (2008) 395–415.
[100] M. Iizasa, H. Suzuki, T. Noguchi, Orientations of carboxylate groups coupled to the Mn cluster in the photosynthetic oxygen-evolving center as studied by polarized ATR–FTIR spectroscopy, Biochemistry 49 (2010) 3074–3082.
[101] M.A. Strickler, H.J. Hwang, R.L. Burnap, J. Yano, L.M. Walker, R.J. Service, R.D. Britt, W. Hillier, R.J. Debus, Glutamate-354 of the CP43 polypeptide interacts with the oxygen-evolving Mn_4Ca cluster of Photosystem II: a preliminary characterization of the Glu354Gln mutant, Philos. Trans. R. Soc. Lond. Ser. B 363 (2008) 1179–1188.
[102] Y. Shimada, H. Suzuki, T. Tsuchiya, T. Tomo, T. Noguchi, M. Mimuro, Effect of a single-amino acid substitution of the 43 kDa chlorophyll protein on the oxygen-evolving reaction of the cyanobacterium *Synechocystis* sp. PCC 6803: analysis of the Glu354Gln mutation, Biochemistry 48 (2009) 6095–6103.
[103] R.J. Service, J. Yano, I. McConnell, H.J. Hwang, D. Niks, R. Hille, T. Wydrzynski, R.L. Burnap, W. Hillier, R.J. Debus, Participation of glutamate-354 of the CP43 polypeptide in the ligation of manganese and the binding of substrate water in Photosystem II, Biochemistry 50 (2011) 63–81.
[104] H.-A. Chu, R.J. Debus, G.T. Babcock, D1-Asp170 is structurally coupled to the oxygen evolving complex in Photosystem II as revealed by light-induced Fourier transform infrared difference spectroscopy, Biochemistry 40 (2001) 2312–2316.
[105] R.J. Debus, M.A. Strickler, L.M. Walker, W. Hillier, No evidence from FTIR difference spectroscopy that aspartate-170 of the D1 polypeptide ligates a manganese ion that undergoes oxidation during the S_0 to S_1, S_1 to S_2, or S_2 to S_3 transitions in Photosystem II, Biochemistry 44 (2005) 1367–1374.
[106] Y. Kimura, N. Mizusawa, A. Ishii, S. Nakazawa, T.-A. Ono, Changes in structural and functional properties of oxygen-evolving complex induced by replacement of D1-glutamate 189 with glutamine in Photosystem II: ligation of glutamate 189 carboxylate to the manganese cluster, J. Biol. Chem. 280 (2005) 37895–37900.
[107] M.A. Strickler, W. Hillier, R.J. Debus, No evidence from FTIR difference spectroscopy that glutamate-189 of the D1 polypeptide ligates a Mn ion that undergoes oxidation during the S_0 to S_1, S_1 to S_2, or S_2 to S_3 transitions in Photosystem II, Biochemistry 45 (2006) 8801–8811.
[108] R.J. Service, J. Yano, D.L. Dilbeck, R.L. Burnap, W. Hillier, R.J. Debus, Participation of glutamate-333 of the D1 polypeptide in the ligation of the Mn_4CaO_5 cluster in Photosystem II, Biochemistry 52 (2013) 8452–8464.
[109] M.A. Strickler, L.M. Walker, W. Hillier, R.D. Britt, R.J. Debus, No evidence from FTIR difference spectroscopy that aspartate-342 of the D1 polypeptide ligates a Mn ion that undergoes oxidation during the S_0 to S_1, S_1 to S_2, or S_2 to S_3 transitions in Photosystem II, Biochemistry 46 (2007) 3151–3160.
[110] J.J. Steenhuis, R.S. Hutchison, B.A. Barry, Alterations in carboxylate ligation at the active site of Photosystem II, J. Biol. Chem. 274 (1999) 14609–14616.
[111] Ö. Saygin, H.T. Witt, On the change of the charges in the four photo-induced oxidation steps of the water-splitting enzyme system S: optical characterization at O_2-evolving complexes isolated from *Synechococcus*, FEBS Lett. 176 (1984) 83–87.
[112] Ö. Saygin, H.T. Witt, Evidence for the electrochromic identification of the change of charges in the four oxidation steps of the photoinduced water cleavage in photosynthesis, FEBS Lett. 187 (1985) 224–226.
[113] H. Kretschmann, E. Schlodder, H.T. Witt, Net charge oscillation and proton release during water oxidation in photosynthesis: an electrochromic band shift study at pH = 5.5–7.0, Biochim. Biophys. Acta 1274 (1996) 1–8.
[114] A. Mulkidjanian, D. Cherepanov, M. Haumann, W. Junge, Photosystem II of green plants: topology of core pigments and redox cofactors as inferred from electrochromic difference spectra, Biochemistry 35 (1996) 3093–3107.
[115] R. Ahlbrink, M. Haumann, D. Cherepanov, O. Bögershausen, A. Mulkidjanian, W. Junge, Function of tyrosine-z in water oxidation by Photosystem II: electrostatical promotor instead of hydrogen abstractor, Biochemistry 37 (1998) 1131–1142.
[116] F. Rappaport, J. Lavergne, Proton release during successive oxidation steps of the photosynthetic water oxidation process: stoichiometries and pH dependence, Biochemistry 30 (1991) 10004–10012.
[117] E. Schlodder, H.T. Witt, Stoichiometry of proton release from the catalytic center in photosynthetic water oxidation — reexamination by a glass electrode study at pH 5.5–7.2, J. Biol. Chem. 274 (1999) 30387–30392.
[118] K. Brettel, E. Schlodder, H.T. Witt, Nanosecond reduction kinetics of photooxidized chlorophyll a_{II} (P-680) in single flashes as a probe for the electron pathway, H^+-release and charge accumulation in the O_2-evolving complex, Biochim. Biophys. Acta 766 (1984) 403–415.
[119] B. Meyer, E. Schlodder, J.P. Dekker, H.T. Witt, O_2 evolution and Chl aII + ($P\text{-}680^+$) nanosecond reduction kinetics in single flashes as a function of pH, Biochim. Biophys. Acta 974 (1989) 36–43.
[120] C. Jeans, M.J. Schilstra, D.R. Klug, The temperature dependence of $P680^+$ reduction in oxygen-evolving Photosystem II, Biochemistry 41 (2002) 5015–5023.
[121] W.C. Liang, T.A. Roelofs, R.M. Cinco, A. Rompel, M.J. Latimer, W.O. Yu, K. Sauer, M.P. Klein, V.K. Yachandra, Structural change of the Mn cluster during the $S_2 \rightarrow S_3$ state transition on of the oxygen-evolving complex of Photosystem II: does it reflect the onset of water/substrate oxidation? Determination by Mn X-ray absorption spectroscopy, J. Am. Chem. Soc. 122 (2000) 3399–3412.
[122] M. Haumann, C. Müller, P. Liebisch, L. Iuzzolino, J. Dittmer, M. Grabolle, T. Neisius, W. Meyer-Klaucke, H. Dau, Structural and oxidation state changes of the Photosystem II manganese complex in four transitions of the water oxidation cycle ($S_0 \rightarrow S_1$, $S_1 \rightarrow S_2$, $S_2 \rightarrow S_3$, and $S_{3,4} \rightarrow S_0$) characterized by X-ray absorption spectroscopy at 20 K and room temperature, Biochemistry 44 (2005) 1894–1908.
[123] Y. Pushkar, J. Yano, K. Sauer, A. Boussac, V.K. Yachandra, Structural changes in the Mn_4Ca cluster and the mechanism of photosynthetic water splitting, Proc. Natl. Acad. Sci. U. S. A. 105 (2008) 1879–1884.
[124] R.J. Service, W. Hillier, R.J. Debus, Evidence from FTIR difference spectroscopy of an extensive network of hydrogen bonds near the oxygen-evolving Mn_4Ca cluster of Photosystem II involving D1-Glu65, D2-Glu312, and D1-Glu329, Biochemistry 49 (2010) 6655–6669.
[125] R.J. Service, W. Hillier, R.J. Debus, A network of hydrogen bonds near the oxygen-evolving Mn_4CaO_5 cluster of Photosystem II probed with FTIR difference spectroscopy, Biochemistry 53 (2014) 1001–1017.
[126] R.J. Debus, Evidence from FTIR difference spectroscopy that D1-Asp61 influences the water reactions of the oxygen-evolving Mn_4CaO_5 cluster of Photosystem II, Biochemistry 53 (2014) 2941–2955.
[127] S.D. Glover, J.C. Goeltz, B.J. Lear, C.P. Kubiak, Mixed valency at the nearly delocalized limit: fundamentals and forecast, Eur. J. Inorg. Chem. (2009) 585–594.
[128] S.D. Glover, J.C. Goeltz, B.J. Lear, C.P. Kubiak, Inter- or intramolecular electron transfer between triruthenium clusters: we'll cross that bridge when we come to it, Coord. Chem. Rev. 254 (2010) 331–345.
[129] C.P. Kubiak, Inorganic electron transfer: sharpening a fuzzy border in mixed valency and extending mixed valency across supramolecular systems, Inorg. Chem. 52 (2013) 5663–5676.
[130] P. Glatzel, U. Bergmann, J. Yano, H. Visser, J.H. Robblee, W. Gu, F.M.F. De Groot, G. Christou, V.L. Pecoraro, S.P. Cramer, V.K. Yachandra, The electronic structure of Mn in oxides, coordination complexes, and the oxygen-evolving complex of Photosystem II studied by resonant inelastic X-ray scattering, J. Am. Chem. Soc. 126 (2004) 9946–9959.
[131] P. Glatzel, H. Schroeder, Y. Pushkar, T. Boro III, S. Mukherjee, G. Christou, V.L. Pecoraro, J. Messinger, V.K. Yachandra, U. Bergmann, J. Yano, Electronic structural changes of Mn in the oxygen-evolving complex of Photosystem II during the catalytic cycle, Inorg. Chem. 52 (2013) 5642–5644.
[132] H.-A. Chu, H. Sackett, G.T. Babcock, Identification of a Mn–O–Mn cluster vibrational mode of the oxygen-evolving complex in Photosystem II by low-frequency FTIR spectroscopy, Biochemistry 39 (2000) 14371–14376.
[133] H.-A. Chu, W. Hillier, N.A. Law, G.T. Babcock, Identification of a possible Mn–O–Mn cluster vibrational mode of the S_3 state in the oxygen-evolving complex of Photosystem II by low-frequency FTIR difference spectroscopy, PS2001 Proceedings: 12th International Congress on Photosynthesis, CSIRO Publishing, Collingwood, Australia, 2001, pp. S13–S027.
[134] Y. Kimura, A. Ishii, T. Yamanari, T.-A. Ono, Water-sensitive low-frequency vibrations of reaction intermediates during S-state cycling in photosynthetic water oxidation, Biochemistry 44 (2005) 7613–7622.
[135] H.-A. Chu, W. Hillier, N.A. Law, G.T. Babcock, Vibrational spectroscopy of the oxygen-evolving complex and of manganese model compounds, Biochim. Biophys. Acta 1503 (2001) 69–82.
[136] Y. Kimura, K. Hasegawa, T. Yamanari, T.-A. Ono, Studies on photosynthetic oxygen-evolving complex by means of Fourier transform infrared spectroscopy: calcium and chloride cofactors, Photosynth. Res. 84 (2005) 245–250.
[137] N. Mizusawa, Y. Kimura, A. Ishii, T. Yamanari, S. Nakazawa, H. Teramoto, T.-A. Ono, Impact of replacement of D1 C-terminal alanine with glycine on structure and function of photosynthetic oxygen-evolving complex, J. Biol. Chem. 279 (2004) 29622–29627.
[138] L.-H. Hou, C.-M. Wu, H.-H. Huang, H.-A. Chu, Effects of ammonia on the structure of the oxygen-evolving complex in Photosystem II as revealed by light-induced FTIR difference spectroscopy, Biochemistry 50 (2011) 9248–9254.
[139] R.D. Britt, J.-L. Zimmermann, K. Sauer, M.P. Klein, Ammonia binds to the catalytic Mn of the oxygen-evolving complex of Photosystem II: evidence by electron spin-echo envelope modulation spectroscopy, J. Am. Chem. Soc. 111 (1989) 3522–3532.
[140] J. Schraut, M. Kaupp, On ammonia binding to the oxygen-evolving complex of Photosystem II: a quantum chemical study, Chem. Eur. J. 20 (2014) 7300–7308.
[141] Y. Shimada, H. Suzuki, T. Tsuchiya, M. Mimuro, T. Noguchi, Structural coupling of an arginine side chain with the oxygen-evolving Mn_4Ca cluster in Photosystem II

as revealed by isotope-edited Fourier transform infrared spectroscopy, J. Am. Chem. Soc. 133 (2011) 3808–3811.
[142] A. Barth, The infrared absorption of amino acid side chains, Prog. Biophys. Mol. Biol. 74 (2000) 141–173.
[143] G. Socrates, Infrared Characteristic Group Frequencies: Tables and Charts, 3rd Edition John Wiley & Sons, Chichester, UK, 2001.
[144] A. Maeda, J. Sasaki, Y. Shichida, Y. Yoshizawa, M. Chang, B. Ni, R. Needleman, J.K. Lanyi, Structures of aspartic acid-96 in the L and N intermediates of bacteriorhodopsin: analysis by Fourier transform infrared spectroscopy, Biochemistry 31 (1992) 4684–4690.
[145] A.K. Dioumaev, Infrared methods for monitoring the protonation state of carboxylic amino acids in the photocycle of bacteriorhodopsin, Biochem. Mosc. 66 (2001) 1269–1276.
[146] B. Nie, J. Stutzman, A. Xie, A vibrational spectral marker for probing the hydrogen-bonding status of protonated Asp and Glu residues, Biophys. J. 88 (2005) 2833–2847.
[147] K.-I. Takei, R. Takahashi, T. Noguchi, Correlation between the hydrogen-bond structures and the C=O stretching frequencies of carboxylic acids as studied by density functional theory calculations: theoretical basis for interpretation of infrared bands of carboxylic groups in proteins, J. Phys. Chem. B 112 (2008) 6725–6731.
[148] F. Siebert, W. Mäntele, W. Kreutz, Evidence for the protonation of two internal carboxylic groups during the photocycle of bacteriorhodopsin, FEBS Lett. 141 (1982) 82–87.
[149] M. Engelhard, K. Gerwert, B. Hess, W. Kreutz, F. Siebert, Light-driven protonation changes of internal aspartic acids of bacteriorhodopsin: an investigation by static and time-resolved infrared difference spectroscopy using [4-^{13}C]aspartic acid labeled purple membrane, Biochemistry 24 (1985) 400–407.
[150] A.K. Dioumaev, H.T. Richter, L.S. Brown, M. Tanio, S. Tuzi, H. Saito, Y. Kimura, R. Needleman, J.K. Lanyi, Existence of a proton transfer chain in bacteriorhodopsin: participation of Glu-194 in the release of protons to the extracellular surface, Biochemistry 37 (1998) 2496–2506.
[151] A.K. Dioumaev, L.S. Brown, R. Needleman, J.K. Lanyi, Fourier-transform infrared spectra of a late intermediate of the bacteriorhodopsin photocycle suggest transient protonation of Asp-212, Biochemistry 38 (1999) 10070–10078.
[152] W.J. de Grip, J. Gillespie, K.J. Rothschild, Carboxyl group involvement in the Meta I and Meta II stages in rhodopsin bleaching: a Fourier transform infrared spectroscopic study, Biochim. Biophys. Acta 809 (1985) 97–106.
[153] U.M. Ganter, W. Gärtner, F. Siebert, Rhodopsin–lumirhodopsin phototransition of bovine rhodopsin investigated by Fourier transform infrared difference spectroscopy, Biochemistry 27 (1988) 7480–7488.
[154] E. Nabedryk, J. Breton, R. Hienerwadel, C. Fogel, W. Mäntele, M.L. Paddock, M.Y. Okamura, Fourier transform infrared difference spectroscopy of secondary quinone acceptor photoreduction in proton transfer mutants of *Rhodobacter sphaeroides*, Biochemistry 34 (1995) 14722–14732.
[155] R. Hienerwadel, S. Grzybek, C. Fogel, W. Kreutz, M.Y. Okamura, M.L. Paddock, J. Breton, E. Nabedryk, W. Mäntele, Protonation of Glu L212 following Q_B^- formation in the photosynthetic reaction center of *Rhodobacter sphaeroides*: evidence from time-resolved infrared spectroscopy, Biochemistry 34 (1995) 2832–2843.
[156] E. Nabedryk, J. Breton, M.Y. Okamura, M.L. Paddock, Proton uptake by carboxylic acid groups upon photoreduction of the secondary quinone (Q_B) in bacterial reaction centers from *Rhodobacter sphaeroides*: FTIR studies on the effects of replacing Glu H173, Biochemistry 37 (1998) 14457–14462.
[157] E. Nabedryk, J. Breton, M.Y. Okamura, M.L. Paddock, Direct evidence of structural changes in reaction centers of *Rb. sphaeroides* containing suppressor mutations for AspL213→Asn: a FTIR study of Q_B photoreduction, Photosynth. Res. 55 (1998) 293–299.
[158] P. Hellwig, B. Rost, U. Kaiser, C. Ostermeier, H. Michel, W. Mäntele, Carboxyl group protonation upon reduction of the *Paracoccus denitrificans* cytochrome *c* oxidase: direct evidence by FTIR spectroscopy, FEBS Lett. 385 (1996) 53–57.
[159] M. Lübben, K. Gerwert, Redox FTIR difference spectroscopy using caged electrons reveals contributions of carboxyl groups to the catalytic mechanism of heme-copper oxidases, FEBS Lett. 397 (1996) 303–307.
[160] P. Hellwig, J. Behr, C. Ostermeier, O.M. Richter, U. Pfitzner, A. Odenwald, B. Ludwig, H. Michel, W. Mäntele, Involvement of glutamic acid 278 in the redox reaction of the cytochrome *c* oxidase from *Paracoccus denitrificans* investigated by FTIR spectroscopy, Biochemistry 37 (1998) 7390–7399.
[161] M. Lübben, A. Prutsch, B. Mamat, K. Gerwert, Electron transfer induces side-chain conformational changes of glutamate-286 from cytochrome bo_3, Biochemistry 38 (1999) 2048–2056.
[162] A. Xie, W.D. Hoff, A.R. Kroon, K.J. Hellingwerf, Glu46 donates a proton to the 4-hydroxycinnamate anion chromophore during the photocycle of photoactive yellow protein, Biochemistry 47 (1996) 14671–14678.
[163] M. Shoji, H. Isobe, S. Yamanaka, Y. Umena, K. Kawakami, N. Kamiya, J.-R. Shen, K. Yamaguchi, Theoretical insight into hydrogen-bonded networks and proton wire for the $CaMn_4O_5$ cluster of Photosystem II. Elongation of Mn–Mn distances with hydrogen bonds, Catal. Sci. Technol. 3 (2013) 1831–1848.
[164] T. Noguchi, M. Sugiura, FTIR detection of water reactions during the flash-induced S-state cycle of the photosynthetic water-oxidizing complex, Biochemistry 41 (2002) 15706–15712.
[165] H. Suzuki, M. Sugiura, T. Noguchi, pH dependence of the flash-induced S-state transitions in the oxygen-evolving center of Photosystem II from *Thermosynechococcus elongatus* as revealed by Fourier transform infrared spectroscopy, Biochemistry 44 (2005) 1708–1718.
[166] H. Suzuki, M. Sugiura, T. Noguchi, Monitoring proton release during photosynthetic water oxidation in Photosystem II by means of isotope-edited infrared spectroscopy, J. Am. Chem. Soc. 131 (2009) 7849–7857.
[167] R. Pokhrel, R.J. Service, R.J. Debus, G.W. Brudvig, Mutation of lysine 317 in the D2 subunit of Photosystem II alters chloride binding and proton transport, Biochemistry 52 (2013) 4758–4773.
[168] C. Tommos, G.T. Babcock, Proton and hydrogen currents in photosynthetic water oxidation, Biochim. Biophys. Acta 1458 (2000) 199–219.
[169] C.A. Wraight, Chance and design — proton transfer in water, channels and bioenergetic proteins, Biochim. Biophys. Acta 1757 (2006) 886–912.
[170] D.N. Silverman, R. McKenna, Solvent-mediated proton transfer in catalysis by carbonic anhydrase, Acc. Chem. Res. 40 (2007) 669–675.
[171] R.L. Mikulski, D.N. Silverman, Proton transfer in catalysis and the role of proton shuttles in carbonic anhydrase, Biochim. Biophys. Acta 1804 (2010) 422–426.
[172] M.Y. Okamura, M.L. Paddock, M.S. Graige, G. Feher, Proton and electron transfer in bacterial reaction centers, Biochim. Biophys. Acta 1458 (2000) 148–163.
[173] M.L. Paddock, G. Feher, M.Y. Okamura, Proton transfer pathways and mechanism in bacterial reaction centers, FEBS Lett. 555 (2003) 45–50.
[174] C.A. Wraight, Intraprotein proton transfer — concepts and realities from the bacterial photosynthetic reaction center, in: M. Wikström (Ed.), Biophysical and Structural Aspects of Bioenergetics, RSC Publishing, Cambridge, UK, 2005, pp. 273–313.
[175] J.L. Lee, J. Reimann, Y. Huang, P. Ädelroth, Functional proton transfer pathways in the heme-copper oxidase superfamily, Biochim. Biophys. Acta 1817 (2012) 537–544.
[176] C. van Ballmoos, P. Ädelroth, R.B. Gennis, P. Brzezinski, Proton transfer in ba_3 cytochrome *c* oxidase from *Thermus thermophilus*, Biochim. Biophys. Acta 1817 (2012) 650–657.
[177] P.R. Rich, A. Maréchal, Functions of the hydrophilic channels in proton motive cytochrome *c* oxidase, J. R. Soc. Interface 10 (2013) 20130813.
[178] M. Hundelt, A.-M.A. Hays, R.J. Debus, W. Junge, Oxygenic Photosystem II: the mutation D1-D61N in *Synechocystis* sp. PCC 6803 retards S-state transitions without affecting electron transfer from Y_Z to P_{680}^+, Biochemistry 37 (1998) 14450–14456.
[179] Z.L. Li, R.L. Burnap, Mutations of basic arginine residue 334 in the D1 protein of Photosystem II lead to unusual S_2 state properties in *Synechocystis* sp PCC 6803, Photosynth. Res. 72 (2002) 191–201.
[180] J. Clausen, R.J. Debus, W. Junge, Time-resolved oxygen production by PSII: chasing chemical intermediates, Biochim. Biophys. Acta 1655 (2004) 184–194.
[181] D.L. Dilbeck, H.J. Hwang, I. Zaharieva, L. Gerencser, H. Dau, R.L. Burnap, The D1-D61N mutation in *Synechocystis* sp. PCC 6803 allows the observation of pH-sensitive intermediates in the formation and release of O_2 from Photosystem II, Biochemistry 51 (2012) 1079–1091.
[182] B.C. Polander, B.A. Barry, Detection of an intermediary, protonated water cluster in photosynthetic oxygen evolution, Proc. Natl. Acad. Sci. U. S. A. 110 (2013) 10634–10639.
[183] T. Noguchi, M. Sugiura, Structure of an active water molecule in the water-oxidizing complex of Photosystem II as studied by FTIR spectroscopy, Biochemistry 39 (2000) 10943–10949.
[184] T. Noguchi, FTIR detection of water reactions in the oxygen-evolving center of Photosystem II, Philos. Trans. R. Soc. Lond. B 363 (2007) 1189–1195.
[185] J. Breton, E. Nabedryk, Proton uptake upon quinone reduction in bacterial reaction centers: IR signature and possible participation of a highly polarizable hydrogen bond network, Photosynth. Res. 55 (1998) 301–307.
[186] F. Garczarek, L.S. Brown, J.K. Lanyi, K. Gerwert, Proton binding within a membrane protein by a protonated water cluster, Proc. Natl. Acad. Sci. U. S. A. 102 (2005) 3633–3638.
[187] F. Garczarek, K. Gerwert, Functional waters in intraprotein proton transfer monitored by FTIR difference spectroscopy, Nature 439 (2006) 109–112.
[188] E. Nabedryk, J. Breton, Coupling of electron transfer to proton uptake at the Q_B site of the bacterial reaction center: a perspective from FTIR difference spectroscopy, Biochim. Biophys. Acta 1777 (2008) 1229–1248.
[189] H. Suzuki, J. Yu, T. Kobayashi, H. Nakanishi, P.J. Nixon, T. Noguchi, Functional roles of D2-Lys317 and the interacting chloride ion in the water oxidation reaction of Photosystem II as revealed by Fourier transform infrared analysis, Biochemistry 52 (2013) 4748–4757.
[190] H. Suzuki, M. Sugiura, T. Noguchi, Monitoring water reactions during the S-state cycle of the photosynthetic water-oxidizing center: detection of the DOD bending vibrations by means of Fourier transform infrared spectroscopy, Biochemistry 47 (2008) 11024–11030.
[191] F.H.M. Koua, Y. Umena, K. Kawakami, J.-R. Shen, Structure of Sr-substituted Photosystem II at 2.1 Å resolution and its implications in the mechanism of water oxidation, Proc. Natl. Acad. Sci. U. S. A. 110 (2013) 3889–3894.
[192] J. Kern, R. Alonso-Mori, R. Tran, J. Hattne, R.J. Gildea, N. Echols, C. Glöckner, J. Hellmich, H. Laksmono, R.G. Sierra, B. Lassalee-Kaiser, S. Koroidov, A. Lampe, G. Han, S. Gul, D. DiFiore, D. Milanthianaki, A.R. Fry, A. Miahnahri, D.W. Schafer, M. Messerschmidt, M.M. Seibert, J.E. Koglin, D. Sokaras, T.-C. Weng, J. Sellberg, M.J. Latimer, R.W. Grosse-Kunstleve, P.H. Zwart, W.E. White, P. Glatzel, P.D. Adams, M.J. Bogan, G.J. Williams, S. Boutet, J. Messinger, A. Zouni, N.K. Sauter, V.K. Yachandra, U. Bergmann, J. Yano, Simultaneous femtosecond X-ray spectroscopy and diffraction of Photosystem II at room temperature, Science 340 (2013) 491–495.
[193] W. Hillier, T. Wydrzynski, Substrate water interactions within the Photosystem II oxygen evolving complex, Phys. Chem. Chem. Phys. 6 (2004) 4882–4889.
[194] L. Konermann, J. Messinger, W. Hillier, Mass spectrometry-based methods for studying kinetics and dynamics in biological systems, in: T.J. Aartsma, J. Matysik (Eds.), Biophysical Techniques in Photosynthesis II, Springer, Dordrecht, The Netherlands, 2008, pp. 167–190.